1

2

3 **AC2P20 selectively kills *M. tuberculosis* at acidic pH by depleting free thiols**

4 Shelby J. Dechow[1], Garry B. Coulson[1], Michael W. Wilson[2], Scott D. Larsen[2], and Robert B.

5 Abramovitch[1*]

6

7 [1]Department of Microbiology and Molecular Genetics, Michigan State University, East Lansing,

8 MI 48824. [2] Vahlteich Medicinal Chemistry Core, College of Pharmacy, University of Michigan,

9 Ann Arbor, MI, 48109.

10

11

12

13

14

15

16 *Corresponding Author:

17 Robert Abramovitch

18 E-mail: abramov5@msu.edu

19 Phone: (517) 884-5416

20 Fax: (517) 353-8957

21

22

23

Abstract

Mycobacterium tuberculosis (Mtb) senses and adapts to host immune cues as part of its pathogenesis. One environmental cue sensed by Mtb is the acidic pH of its host niche in the macrophage phagosome. Disrupting the ability of Mtb to sense and adapt to acidic pH has the potential to reduce survival of Mtb in macrophages. Previously, a high throughput screen of a ~220,000 compound small molecule library was conducted to discover chemical probes that inhibit Mtb growth at acidic pH. The screen discovered chemical probes that kill Mtb at pH 5.7 but are inactive at pH 7.0. In this study, AC2P20 was prioritized for continued study to test the hypothesis that it was targeting Mtb pathways associated with pH-driven adaptation. RNAseq transcriptional profiling studies showed AC2P20 modulates expression of genes associated with redox homeostasis. Gene enrichment analysis revealed that the AC2P20 transcriptional profile had significant overlap with a previously characterized pH-selective inhibitor, AC2P36. Like AC2P36, we show that AC2P20 kills Mtb by selectively depleting free thiols at acidic pH. Mass spectrometry studies show the formation of a disulfide bond between AC2P20 and reduced glutathione, supporting a mechanism where AC2P20 is able to deplete intracellular thiols and dysregulate redox homeostasis. The observation of two independent molecules targeting free thiols to kill Mtb at acidic pH further supports that Mtb has restricted redox homeostasis and sensitivity to thiol-oxidative stress at acidic pH.

44 ***Introduction***

45 Mtb pathogenesis is driven by its ability to exploit and adapt to the intracellular host
46 environment. During pathogenesis, Mtb encounters a variety of stressors including nitrosative,
47 oxidative, acidic pH, and hypoxic stress [1]. In response to these stresses, Mtb alters its physiology
48 in order to survive the hostile macrophage environment and modulate expression of virulence
49 genes critical for its pathogenicity. Acidic pH is an initial environmental cue that Mtb senses upon
50 infection of the host macrophage [2,3]. For survival within the resting macrophage, Mtb inhibits
51 fusion of the phagosome and lysosome and resides in a mildly acidic phagosome (pH 6.4) [4].
52 Activation of the macrophage leads to phagosome acidification and Mtb resists this acid stress,
53 maintaining a relatively neutral cytoplasmic pH, even at pH <5.0 [5-8]. In addition to expressing
54 mechanisms to survive acid stress, Mtb also exhibits pH-and-carbon source dependent growth
55 adaptations. Mtb will completely arrest its growth in minimal media buffered to pH 5.7 with
56 glycerol as the sole carbon source [9]. During this growth arrest, Mtb exhibits carbon specificity,
57 and will only arrest growth on glycolytic carbon sources (i.e. glucose and glycerol) [9]. However,
58 when given specific carbon sources (i.e. phosphoenolpyruvate, pyruvate, acetate, oxaloacetate, and
59 cholesterol), Mtb resuscitates its growth at pH 5.7 in minimal media, and thus, exhibits direct
60 metabolic remodeling during pH stress [9]. Collectively, these studies show that in response to
61 acidic pH, Mtb has multiple mechanisms in place whereby it alters its physiology for survival and
62 virulence.

63 When Mtb is cultured at acidic pH or in macrophages, the bacterium has an imbalanced
64 redox state with a more reduced cytoplasm [9,10], a phenomenon referred to as reductive stress
65 [3,11]. It is hypothesized that acidic pH may cause redox imbalances due to adaptations of the
66 electron transport chain that promote oxidative phosphorylation while maintaining cytoplasmic

67 pH homeostasis [3]. These adaptations could lead to an accumulation of reduced co-factors such
68 as NADH/NADPH. Implications for this type of reductive stress included altered Mtb metabolism,
69 slowed growth, and non-replicating persistence. Fatty acid synthesis is thought to help mitigate
70 reductive stress via the oxidation of NADPH and is supported by the induction of genes associated
71 with lipid metabolism and anaplerosis at low pH [2,3,9,12]. One of these induced genes is WhiB3,
72 a regulatory protein that senses Mtb's intracellular redox state through its [4Fe-4S] cluster and acts
73 to mitigate reductive stress [11,13,14]. WhiB3 is thought to counter this reductive stress via its
74 role as a metabolic regulator, whereby it controls the anabolism of virulence lipids: poly- and
75 diacyltrehalose (PAT/DAT), phthiocerol dimycocerosate (PDIM), and sulfolipids (SL-1) [14].
76 Production of these methyl-branched polar lipids requires NADPH; therefore, WhiB3 helps
77 alleviate reductive stress by channeling excess reductants into fatty acid synthesis [14]. This results
78 in the re-oxidation of reducing equivalents needed to maintain intracellular redox homeostasis.
79 Changes in central metabolism, including the induction of anaplerotic pathways driven by
80 isocitrate lyases (*icl*) and phosphoenolpyruvate carboxykinase (*pckA*) at acidic pH [15], and the
81 dependence on carbon sources that feed the anaplerotic node [9], may also provide metabolic
82 flexibility required to balance redox homeostasis at acidic pH.

83 Mechanisms important for pH adaptation (i.e. metabolism, cytoplasmic pH-homeostasis,
84 and redox homeostasis) present an attractive source of novel targetable physiologies for drug
85 discovery. pH homeostasis can be targeted by compounds like the benzoxazinone, BO43, which
86 inhibits the serine protease MarP, resulting in the disruption of intrabacterial pH homeostasis [16].
87 Additionally, ionophores have also been discovered to kill Mtb at acidic pH [17,18]. Respiration
88 has been shown to be important for maintaining pH-homeostasis [19,20]. Compounds targeting
89 respiration include Bedaquiline (BDQ), a F_1F_o-ATP-synthase inhibitor, and the small molecule,

90 C10. BDQ has been shown to act as an ionophore and disrupt the Mtb transmembrane pH gradient
91 [21], while C10 exhibits enhanced Mtb killing at acid stress [22]. Thiol-redox homeostasis also
92 has implications as a targetable pH-dependent physiology. Auranofin depletes free thiols by
93 targeting an essential thioredoxin reductase (TrxB2) [23,24]. Together, these results demonstrate
94 the druggability of physiologies important for acidic pH-dependent adaptation.

95 PhoPR, a two-component regulatory system (TCS), is important for regulating Mtb
96 virulence and intracellular survival [25,12,26]. Additionally, signaling from PhoPR has been
97 shown to play an important role in pH adaptation [2,27,9]. Our lab previously conducted a reporter
98 based, whole cell high-throughput screen (HTS) of > 220,000 small molecules for inhibitors of
99 PhoPR signaling at acidic pH [28,29]. Compound activity was assessed in rich media buffered to
100 pH 5.7 using a pH-inducible Mtb fluorescent reporter strain to identify either direct inhibitors of
101 the PhoPR regulon or pH-selective inhibitors of Mtb growth. This screen successfully identified
102 inhibitors of *phoPR*-dependent signaling, including the carbonic anhydrase (CA) inhibitor,
103 ethoxzolamide (ETZ) [28]. This screen also identified compounds that selectively kill Mtb at pH
104 5.7 but not pH 7.0 and do so independently of PhoPR. One of these compounds, called AC2P36
105 (5-chloro-N-(3-chloro-4-methoxyphenyl)-2-methylsulfonylpyrimidine-4-carboxamide) [29],
106 functions by directly depleting intracellular Mtb thiol pools, by forming covalent adducts with free
107 thiols. Depletion of free thiols, interferes with redox buffering pathways and induces formation of
108 cytoplasmic reactive oxygen species (ROS) at acidic pH, thus sensitizing Mtb to thiol-oxidative
109 stress [29]. AC2P36 also selectively kills Mtb and potentiates the activity of TB drugs: isoniazid,
110 clofazimine, and diamide. We hypothesize that reductive stress at acidic pH selectively sensitizes
111 Mtb to thiol targeting activity of AC2P36. These results indicate that free thiols are a pH-selective
112 target, and that Mtb sensitivity to killing is enhanced under thiol oxidative stress.

113 In this study, we report on a new chemical probe isolated from a prior screen, AC2P20 (N-
114 1,3-benzothiazol-2-yl-2-[(4,6-dioxo-5-phenyl-1,4,5,6-tetrahydropyrimidin-2-yl)thio]acetamide)
115 (Figure 1A), that selectively kills Mtb at acidic pH. AC2P20 was identified as a *phoPR*-
116 independent, pH-selective inhibitor of Mtb growth. Through transcriptional profiling we observed
117 that genes modulated by AC2P20 treatment significantly overlap with genes modulated by
118 AC2P36 treatment. Although both compounds are structurally distinct, like AC2P36, AC2P20 also
119 exhibits killing of Mtb at pH 5.7, disrupts thiol homeostasis by depleting intracellular free thiol
120 pools, and increases reactive oxygen ROS production. Thus, AC2P20 is a second structurally
121 unique pH-selective chemical probe that exhibits thiol-depletion as a mechanism-of-action for
122 killing at acidic pH. This finding further reinforces the vulnerability of Mtb to perturbations of
123 redox homeostasis at acidic pH.
124
125 **Experimental**
126 ***Bacterial Strains and Growth Conditions***
127 *M. tuberculosis* strains Erdman and CDC1551 and *M. smegmatis* strain mc^{2}155 (expressing GFP
128 from a replicating plasmid) were used in all experiments unless specified. Mtb was cultured in
129 Middlebrook 7H9 media enriched with 10% oleic acid-albumin-dextrose-catalase (OADC), 0.05%
130 Tween-80, and glycerol. Cultures were maintained in vented T-25 culture flasks and grown at 37
131 °C and 5% CO_2. To maintain a specific pH, 7H9 media was strongly buffered to pH 7.0 with 100
132 mM 3-(N-morpholino)propanesulfonic acid (MOPS) or pH 5.7 with 100 mM 2-(N-
133 morpholino)ethanesulfonic acid (MES). Mtb was grown to mid-late log phase (OD_{600} 0.5-1.0)
134 before exposure to buffered 7H9 for use in experiments detailed below. *M. smegmatis* cultures

135 were grown in identical 7H9 media conditions at a starting OD_{600} 0.05 at 37°C in a shaking
136 incubator (200 rpm).
137
138 ***Selection for AC2P20 resistant mutants***
139 Mtb CDC1551 and Mtb Erdman strains were grown to an OD_{600} of 0.6-1.0, spun down, and
140 resuspended in 7H9 media buffered to pH 5.7. Mtb cells were plated at 10^9 cells/mL on 7H10 agar
141 media buffered to pH 5.7 and supplemented with 10 µM, 20µM or 40 µM AC2P20. Plates were
142 incubated at 37°C for over 12 weeks without any significant isolated colonies appearing. This
143 experiment was performed three times with similar results.
144
145 ***Transcriptional profiling and data analysis***
146 Mtb cultures were grown at 37°C and 5% CO_2 in standing T-25 culture flasks to an OD_{600} of 0.5
147 in 8 mL of 7H9 buffered media. Treatment conditions examined include i) 20µM AC2P20 at pH
148 5.7 and ii) an equivalent volume of DMSO at pH 5.7 as the baseline control. Each culture was
149 incubated for 24 hours and treatment conditions were conducted in two biological replicates.
150 Following incubation, total bacterial RNA was extracted as previously described [2,9] and
151 sequencing data was analyzed using SPARTA (ver. 1.0) [30]. Genes identified filtered based on
152 $\log_2$CPM < 5 and $\log_2$FC < 1. A Chi-Square analysis with Yates Correction was conducted to test
153 the statistical relationship between gene overlap with the AC2P36 transcriptional profile as
154 described by Coulson *et al.* [29]. The RNAseq data has been deposited at the GEO database
155 (Accession # GSE151884).
156

157 ***Half-maximal effective concentration (EC_{50}) determination and spectrum of activity in other***
158 ***mycobacteria***

159 Mtb cultures were incubated in buffered 7H9 media (pH 5.7 or pH 7.0) at a starting OD_{600} of 0.2,
160 with 200 uL aliquoted into 96-well microtiter assay plates (CoStar #3603). Cultures were treated
161 with a 2.5-fold dose-response of AC2P20 (80 µM-0.13 µM) and incubated standing for 6 days at
162 37 °C and 5% CO_2, with bacterial growth assessed by optical density (OD_{600}). Cultures treated
163 with an equivalent volume of DMSO or 0.3 µM Rifampin were used as negative and positive
164 controls, respectively. Each condition was performed in duplicate and representative of three
165 individual experiments. EC_{50} values were determined using GraphPad Prism software (ver. 7.0).
166 AC2P20 activity against *M. smegmatis* was also performed in 96-well assay plates in 7H9 buffered
167 media (pH 7.0 or 5.7). *M. smegmatis* cultures were seeded at a starting OD_{600} of 0.05 with 200 uL
168 aliquoted into each well. An 8-point 2.5-fold dilution series starting at 80 µM was conducted and
169 cultures were incubated for 3 days with shaking (100 rpm). Plates were read for GFP fluorescence.
170

171 ***Mycobactericidal activity of AC2P20***

172 Mtb was initially cultured in 7H9 media (pH 5.7 or 7.0) at a starting OD_{600} of 0.2 in 96-well assay
173 plates. Cultures were treated with a 2.5-fold dose-response of AC2P20 (80 µM-0.33 µM). An
174 equivalent volume of DMSO was included as a control. Each treatment condition was conducted
175 in triplicate and incubated for 7 days. Following incubation, treated wells were serially diluted in
176 1X Phosphate-Buffered Saline (PBS) and plated for colony forming units (CFUs) on 7H10 agar
177 plates supplemented with 10% OADC and glycerol. Bactericidal activity was determined by
178 comparing CFUs from the initial inoculum to CFUs following treatment.
179

180 ***Cytoplasmic pH-homeostasis***

181 Mtb washed with PBS (pH 7.0) was labelled with Cell Tracker 5'-chloromethylfuoroscein
182 diacetate (CMFDA) and analyzed using methods previously described [31]. Mtb treated with
183 AC2P20 in PBS (pH 5.7) was assayed for cytoplasmic pH changes over the course of 24-hours.
184 Excitation ratio results were converted to pH via a standard curve generated using Nigericin-
185 treated Mtb in buffers of known pH. Treated Mtb results were then compared to the DMSO and
186 Nigericin negative and positive controls, respectively.

187

188 ***Measurement of endogenous reactive oxygen species***

189 CellROX Green fluorescent dye (Invitrogen) was used to detect accumulation of endogenous
190 reactive oxygen species (ROS) in Mtb as previously reported [29,32]. Mtb grown to mid-late log
191 phase was pelleted and re-suspended at a starting OD_{600} of 0.5 in 5 mL of buffered 7H9 media (pH
192 5.7 or 7.0) lacking catalase. Cultures prepared in duplicate were treated with two separate
193 concentrations of AC2P20 (2 μM and 20 μM) and incubated for 24 hours at 37 °C. Following
194 treatment, cultures were incubated with 5 mM CellROX Green (Thermo Fisher) for 1 hour at 37
195 °C and then washed twice with 1X PBS + 0.05% Tween80. Washed cells were resuspended in 0.6
196 mL 1X PBS and aliquoted into triplicate wells in 96-well microtiter plates. Wells were measured
197 for fluorescence and optical density, with florescence being subsequently normalized to cell
198 growth for ROS analysis. AC2P36 (2 μM and 20 μM) and equivalent volumes of DMSO served
199 as positive and baseline controls, respectively.

200

201

202

203 ***Detecting intracellular free thiol pools***

204 Mtb grown in 7H9 OAD media lacking catalase was inoculated at a starting OD_{600} of 0.25 in 8 mL
205 of buffered 7H9 OAD media (pH 5.7 or 7.0) also lacking catalase. Cultures were prepared in
206 duplicate and treated with either DMSO, 2 μM AC2P20, 20 μM AC2P20, 20 μM AC2P36, or 20
207 μM auranofin. Treated cultures were incubated for 24 hours at 37 °C, normalized by OD_{600}, and
208 washed twice in 1X PBS supplemented with 0.05% Tyloxapol. Cells were resuspended in 0.75
209 mL of thiol assay buffer (100 mM potassium phosphate pH 7.4, and 1 mM EDTA) and lysed by
210 bead beating for 2 minutes at room temperature. Supernatants were removed and saved for analysis
211 using the Cayman Thiol Detection Assay Kit (Caymen Chemical) as previously described [29].
212 Thiol concentrations were measured in (nM) against a glutathione standard.

213

214 ***Mass Spectrometry***

215 Mass spectrometry was used to detect the formation of AC2P20 adducts. Aqueous solutions of 80
216 μM AC2P20 were prepared separately and incubated with either reduced glutathione (100 μM),
217 N-acetylcysteine (100 μM), or hydrogen peroxide (100 μM) for 1 hour at room temperature in
218 Tris-HCl buffer (pH 5.7, 7.0, or 8.5). Samples were analyzed using the Waters Xevo G2-XS QTof
219 mass spectrometer (Milford, MA, USA) in both positive and negative electrospray ionization (ESI)
220 modes. Samples were run with the following ion source parameters: capillary voltage, 2 kV;
221 sampling cone, 35 V; source temperature, 100°C; desolvation temperature, 350°C; cone gas flow,
222 25 L/h; desolvation gas flow, 600 L/h. Ultra-performance liquid chromatography (UPLC), using
223 water and acetonitrile as solvents, was carried out for the chromatographic separation of
224 compounds. The LC parameters were as follows: flow rate, 0.2 mL/min; water/acetonitrile solvent

225 gradient, 50/50 for 2 min. Mass analysis was performed at <1,500 Da. This experiment was
226 repeated twice in duplicate with similar results seen at both positive and negative ESI.
227
228 **Results**
229 ***AC2P20 exhibits pH-dependent growth inhibition of M. tuberculosis.*** Two high throughput
230 screens (HTS) using Mtb fluorescent reporters were conducted in order to detect inhibitors of two
231 separate Mtb two-component regulatory systems (TCS): DosRST and PhoPR [28,29,33,34]. A
232 chemical library of >220,000 small molecules was previously screened, with compound hits being
233 defined as those that inhibited reporter fluorescence or Mtb growth. These compounds were further
234 classified as TCS target inhibitors or growth inhibitors. The screens only differed in the reporter
235 strain used and the pH of the medium, which was neutral or acidic in the DosRST and PhoPR
236 inhibitor screens, respectively. Comparing growth inhibiting hits from these two screens identified
237 a subset of compounds that selectively inhibited Mtb growth at acidic pH independent of PhoPR
238 signaling. These compounds were classified as pH-selective growth inhibitors if they exhibited
239 >50% growth inhibition at acidic pH and < 10% inhibition at neutral pH. AC2P20 (N-1,3-
240 benzothiazol-2-yl-2-[(4,6-dioxo-5-phenyl-1,4,5,6-tetrahydropyrimidin-2-yl)thio]acetamide)
241 (Figure 1A) exhibited >5-fold selectivity at acidic pH and was characterized as one of these pH-
242 selective inhibitors of Mtb growth. The pH-dependent activity of AC2P20 was confirmed by
243 determining its half-maximal effective concentration (EC_{50}). Mtb treated with an 8-point dose-
244 response of AC2P20 for six days at pH 5.7 results in dose-dependent growth inhibition with an
245 EC_{50} of 4.3 μM, however, has a >10-fold higher EC_{50} of ~60 μM at pH 7.0 (Figure 1B). AC2P20
246 also exhibits mycobacterial selectivity for Mtb compared to *M. smegmatis*, which has an EC_{50} >
247 80 μM at acidic pH and does not exhibit growth inhibitory activity at neutral pH (Figure S1A).

248 Time-dependent and concentration-dependent killing assays were conducted to define whether
249 AC2P20 is bactericidal or bacteriostatic. Mtb treated with 20 μM AC2P20 exhibits pH-selective
250 inhibition of Mtb growth in acidic conditions and results in approximately 2-log fold reduction in
251 CFUs over 5 days (Figure 1C). In contrast, DMSO controls and AC2P20 treatment in neutral
252 conditions have no impact on growth. The concentration-dependent killing assay shows that
253 AC2P20 is bactericidal at ~32 μM and bacteriostatic at 12 μM (Figure 1D). Cytoplasmic pH was
254 measured to determine whether AC2P20 functions as an ionophore. Treatment with AC2P20 does
255 not modulate the cytoplasmic pH of Mtb compared to the nigericin positive control (Figure S1B).
256 Together, these data show that AC2P20 activity is pH-dependent, bactericidal, and does not alter
257 Mtb cytoplasmic pH homeostasis.
258
259 ***AC2P20 induces a thiol oxidative stress response similar to AC2P36***. To isolate resistant mutants
260 and thereby find potential targets for AC2P20, 10^9 Mtb cells were plated on 7H10 agar media
261 buffered to pH 5.7 containing 10 μM, 20 μM or 40 μM AC2P20. Despite several weeks of
262 incubation each time at 37°C, no spontaneous mutants were isolated from multiple rounds of
263 screening for resistant mutants to AC2P20. Following our resistance screening attempts,
264 transcriptional profiling was conducted to define Mtb physiologies targeted following AC2P20
265 treatment. Mtb CDC1551 cultures were prepared in rich media (pH 5.7) and treated with 20μM
266 AC2P20 or DMSO control for 24 hours. Mtb treated with AC2P20 caused induction of 156 genes
267 (>2-fold, $q < 0.05$) and repression of 81 genes (>2-fold, $q < 0.05$) (Figure 2A, Table S1). Using
268 MycoBrowser [35] to classify gene function, we found that the functional pathway most induced
269 by AC2P20 (excluding conserved hypotheticals) was intermediary metabolism and respiration
270 (Figure 2B, Table S1A, Table S1B). Differentially induced genes included genes involved in sulfur

271 metabolism (*cysT, sirA, mec*), transcriptional regulation of the stress response (*sigH, sigB, rshA*),
272 and redox homeostasis (*katG, trxB1, trxC*) (Figure 2C, Table S1B). Notably, differentially
273 regulated genes from AC2P20 treated cells overlapped with differential gene expression profiles
274 previously characterized for the pH-selective Mtb growth inhibitor, AC2P36 [29]. Gene
275 enrichment analysis showed a statistically significant overlap between groups AC2P20 and
276 AC2P36 differentially expressed genes ($p<0.0001$) (Figure 2C). Based on RNAseq data and the
277 gene enrichment analysis, both AC2P36 and AC2P20 exhibit a transcriptional profile indicative
278 of redox and thiol-oxidative stress. For example, both transcriptomes show induction of the
279 alternative sigma factor *sigH* regulon which plays a central role in regulating thiol-oxidative stress
280 during Mtb pathogenesis [36-38]. *sigH* is responsible for regulating genes involved in thiol
281 metabolism including thioredoxin (*trxC*), thioredoxin reductases (*trxB1, trxB2*), and cysteine
282 biosynthesis and sulfate transport (*cysO*, *cysM, cysA, cysW, cysT*). Additionally, *sigH*-regulated
283 *moeZ* is induced in both transcriptomes, which is involved in sulfation of enzymes and plays a
284 dual role in molybdopterin biosynthesis and *cysO* activation[39]. While the *sigH* regulon exhibits
285 a direct response to thiol-oxidative stress, it is also highly induced under oxidative stress
286 conditions[36]. In addition, non-*sigH* regulated oxidative stress responsive genes include *katG*
287 (catalase-peroxidase), *thiX* (a thioredoxin), and *furA* (transcriptional regulator), which are
288 upregulated in both AC2P20 and AC2P36. Interestingly, *Rv0560c*, a methyltransferase, is the most
289 upregulated gene in Mtb treated with AC2P20, AC2P36, or C10 [22,29]. *Rv0560c* is induced in
290 mutants resistant to a cyano-substituted fused pyrido-benzimidazole, known as compound 14, and
291 provides resistance by methylating and inactivating compound 14 [40]. *Rv0560c* is not directly
292 upregulated by the *sigH* regulon or oxidative stress, but rather by salicylate [41], and may be
293 involved in the synthesis of redox cycling agents [42-44]. Therefore, induction of thiol-

294 homeostasis metabolism genes and *katG* in response to AC2P20 treatment suggests an increased
295 need for the generation of low molecular weight thiols, which are important for detoxification of
296 toxic reactive oxygen species (ROS) and maintaining redox homeostasis in Mtb.

297 Despite significant overlap between the AC2P20 and AC2P36-treated regulons, there are
298 pathways that are distinctly different in the transcriptional profiling comparisons. Classification of
299 gene function for the 180 AC2P36-induced genes (>2-fold, $q < 0.05$) showed that the functional
300 category most induced (excluding conserved hypotheticals) was intermediary metabolism and
301 respiration, the same as AC2P20. However, major differences were noted between categories of
302 both induced gene sets for AC2P20 and AC2P36. For example, induction of lipid metabolism
303 genes comprised roughly 3.33% of the total genes induced by AC2P36 compared to 12.82% for
304 AC2P20 (Figure 2B, Figure S2A). Noticeably, AC2P20 appeared to upregulate several mycolic
305 acid biosynthesis pathway and operon genes (*fas, acpM, kasA, accD6*) (Figure S2B). In contrast,
306 these genes were repressed following AC2P36 treatment. Other lipid metabolism genes not
307 observed in AC2P20 transcriptional data, but actively repressed by AC2P36 include *scoA/B*,
308 *accD1*, *Rv3087*, and *fadE35 [29]*. Additionally, transcriptional profiling showed that methylcitrate
309 synthase and methylcitrate dehydratase genes (*prpC* and *prpD*, respectively) were oppositely
310 modulated in both regulons; AC2P20 repressed *prpC/D* expression while their expression was
311 induced by AC2P36 (Figure S2B). Other functional categories that saw large quantitative changes
312 between both transcriptional profiles include cell wall and cell wall processes and virulence,
313 detoxification and adaptation. Fewer cell wall and cell wall processes genes were induced by
314 AC2P36 compared to AC2P20, while the number of virulence, detoxification and adaptation
315 functional genes were increased following AC2P36 treatment (Figure S2A). The transcriptional
316 differences observed between both regulons demonstrates that despite the shared similarities in

317 regulation of thiol-redox homeostasis and regulatory genes, distinct differences exist between how
318 pathways are modulated following AC2P20 and AC2P36, with lipid metabolism being most
319 notable.
320
321 ***AC2P20 forms an adduct with the low molecular weight thiol, GSH.*** Although AC2P36 and
322 AC2P20 have distinct structures, both compounds contain a similar thiol-containing pyrimidine
323 group. In AC2P36, it is thought that the methylsulfone moiety acts as an electron-withdrawing
324 group which allows a thiolate anion to undergo nucleophilic attack on the C-2 carbon of the
325 pyrimidine ring in order to release methanesulfinic acid or methanesulfinate (Figure S1C) [29].
326 This interaction is thought to result in the formation of a sulfide bond and depletion of available
327 free thiols. Indeed, heteroaromatic sulfones have been recently described as tunable agents for
328 cysteine-reactive profiling [45,46]. Based on these observations with AC2P36, and the noted
329 similarity with the thiol-containing pyrimidine group, we hypothesized that AC2P20 may have a
330 similar mechanism of action and undergo covalent modification of free thiols. To test this
331 hypothesis, 80μM AC2P20 was incubated with 100μM reduced glutathione (GSH) for one hour
332 in basic, neutral, and acidic conditions and analyzed via mass spectrometry. Incubation of AC2P20
333 with GSH resulted in the formation of an adduct at pH 5.7 with an exact molecular weight of ~529
334 Da (Figure 3A, Figure 3C, Figure S5). There is also adduct formation in neutral and basic
335 conditions (Figure S3A, Figure S3B) although with lower peak intensity. AC2P20 incubated with
336 DMSO does not appear to fragment in the absence of GSH in any of these conditions. (Figure 3B,
337 Figure S3C, Figure S3D). In the positive ESI mode (Figure 3C), a neutral fragment of 129 Da is
338 lost from the adduct with a peak seen at ~401 Da, consistent with a loss of the glutamate fragment
339 from GSH [47]. Fragmentation of AC2P20 is also observed when incubated with GSH at pH 5.7,

340 with peaks at ~222 Da, ~206 Da, ~194 Da, and ~178 Da aligning with possible fragments of the
341 pyrimidine group of AC2P20 (Figure S5). The peak observed at ~391 Da is a mass spectrometry
342 plasticizer and common contaminant that can be used for mass calibration [48]. We also looked at
343 N-acetylcysteine (NAC), a derivative of GSH, and its ability to form an adduct with AC2P20. A
344 peak was observed at ~384 Da, aligning with the formation of an AC2P20-NAC adduct (Figures
345 S4A, Figure S5). Interestingly, higher peak intensities of these adducts were observed at neutral
346 and basic conditions (Figure S4B, Figure S4C). This is possibly due to NAC having a pKa ~9.5,
347 and therefore favoring the adduct reaction with AC2P20 under these conditions. Together, these
348 findings support that AC2P20 reacts with low molecular weight thiols and thiol groups.
349 Additionally, we looked at whether AC2P20 still form an adduct with GSH in the presence of the
350 oxidant, H_2O_2. It was thought that H_2O_2 may cause the formation of intermediate sulfenic acid and
351 oxidize GSH, resulting in the formation of glutathione (GSSG) [49]. After incubating AC2P20
352 with both GSH and H_2O_2, we still observed disulfide bond formation between AC2P20 and GSH,
353 indicating that GSSG is probably not being produced (Figure S4D). These results suggest that
354 AC2P20 is capable of forming a disulfide bond with low molecular weight thiols.
355
356 ***AC2P20 depletes free thiols and causes an accumulation in ROS in Mtb at acidic pH.*** Given that
357 an adduct is able to form between AC2P20 and GSH, we sought to test the ability of AC2P20 to
358 deplete free thiols in Mtb. For this assay, Mtb was treated with AC2P20 (2 μM and 20 μM) in both
359 acidic and neutral conditions for 24 hours. Auranofin (20 μM) was used as a positive control
360 because it inhibits Mtb's thioredoxin reductase, TrxB2, thereby disrupting thiol- and redox-
361 homeostasis[23]. AC2P36 (20 μM) was also included in the assay to compare thiol depleting
362 activities of both compounds. Following AC2P20 treatment, a statistically significant reduction in

363 free thiol concentrations was observed intracellularly in Mtb at pH 5.7 where free thiols are
364 reduced by ~2.8-fold to ~133nM compared to the DMSO vehicle control at ~380 nM (Figure 4A).
365 As expected, we also see free thiol depletion in Mtb following treatment with both positive
366 controls, supporting the observation seen with AC2P20. In contrast to Auranofin, AC2P20
367 treatment at neutral pH does not exhibit any statistically significant reduction in free thiols,
368 supporting the pH-selective activity of this compound. Interestingly, AC2P36 does exhibit some
369 activity in neutral conditions. This is possibly due to AC2P36 still exhibiting some growth
370 inhibitory activity at neutral pH at ~30 μM, whereas AC2P20 requires much higher concentrations
371 (~60 μM) to see a similar inhibitory effect.

372 Depletion of total free thiols will result in disrupted redox homeostasis and therefore may
373 result in enhanced ROS accumulation. To test this hypothesis, we conducted an assay measuring
374 intracellular ROS production in Mtb. Mtb was incubated with 2 μM and 20 μM AC2P20 for 24
375 hours, treated with CellROX fluorescent dye for 1 hour, and then assayed for relative fluorescence
376 and optical density. AC2P36 (2 μM and 20 μM) was included as the positive control, because it
377 has previously been shown to accumulate intracellular ROS following treatment. At acidic pH, 20
378 μM AC2P20 exhibits ~3-fold increase in intracellular ROS production compared to DMSO (Figure
379 4B). AC2P20 (20 μM) also increases ROS accumulation ~3-fold greater in acidic conditions
380 compared to neutral pH, where there is little ROS accumulation compared to DMSO. AC2P36 (20
381 μM) also increases ROS production ~2-fold at pH 5.7, which is consistent with previous
382 observations. These data support a mechanism whereby enhanced ROS accumulation can be
383 driven by pH stress and is further exacerbated by AC2P20 treatment.

384

385

386 ***Discussion***

387 Based on the chemical structure of AC2P20 and the adduct it forms with GSH at pH 5.7,
388 we propose a reaction model where the benzothioazole-mercaptoacetamide group covalently
389 modifies free thiols, forming stable adducts. Shown here is a potential mechanism for the
390 generation of adducts observed by mass spectrometry (Figure 3A, Figure 3C). Disulfide bond
391 formation between GSH (307.32 Da) and the free benzothioazole-mercaptoacetamide group
392 (223.29 Da) results in a molecule mass of 529 Da, which can be observed in both positive and
393 negative ESI modes (Figure 5A, Figure S5). Loss of the neutral glutamate fragment from the
394 AC2P20-GSH adduct results in a peak at 401 Da (ESI+). We suspect AC2P20 may be undergoing
395 hydrolysis, however, we do not observe the phenyl-dioxopyrimidine fragment (204 Da). We do
396 observe a fragmented phenyl-dioxopyrimidine group at 178 Da which may be due to the sample's
397 molecules breaking into charged fragments during mass spectrometry. The absence of a 204 Da
398 fragment may also suggest that adduct formation could be occurring via a different chemical
399 process. However, the observation of an adduct supports that the formation of disulfide bonds
400 between AC2P20 and other thiol-containing molecules could be occurring in Mtb (Figure 5B).

401 Although, both AC2P20 and AC2P36 function by depleting free thiols, the two scaffolds
402 are distinctly different and engage glutathione (GSH) in different ways. AC2P36 is itself an
403 electrophile, by virtue of the reactive methanesulfonyl moiety on the pyrimidine. GSH can add
404 directly to AC2P36 on the pyrimidine, followed by elimination of the excellent leaving group
405 methanesulfinic acid[29]. On the other hand, AC2P20 is not itself reactive to GSH in an analogous
406 fashion, as evidenced by a lack of MS ion for a direct adduct of GSH to the pyrimidine dione
407 moiety. Instead, AC2P20 has to get hydrolyzed to the free thiol, after which it forms a disulfide

408 with GSH. Therefore, AC2P20 and AC2P26 have different chemical mechanisms of action, and
409 the GSH adducts are chemically distinct (*e.g.* disulfide vs thiopyrimidine).

410 Redox homeostasis represents a potentially important Mtb vulnerability at acidic pH. Mtb
411 experiences reductive stress during hypoxia and at acidic pH [10]. Genes important for mitigating
412 redox stress are shown to be directly influenced by acid stress; therefore, disruption of redox
413 homeostasis results in the loss of Mtb protection against acid stress [10]. Furthermore, direct
414 perturbations to either redox-homeostasis or pH-homeostasis results in decreased drug tolerance
415 and enhanced Mtb killing [50]. Indeed, chloroquine has recently been shown to kill Mtb *in vivo* by
416 targeting redox homeostasis [50] and auranofin also shows promising antimycobacterial activity
417 [23,51]. Furthermore, agents targeting respiration may similarly have activity by promoting redox
418 imbalance. Thus, targeting redox-homeostasis represents an important new approach to treating
419 TB. Like AC2P36, we have discovered a second, albeit novel, pH-selective compound (AC2P20)
420 that directly targets free thiols to perturb redox homeostasis. Both AC2P36 and AC2P20 deplete
421 free thiol pools and increase intracellular ROS as part of their killing mechanisms. Interestingly,
422 AC2P20 depletes less free thiols than AC2P36, but has a greater increase in intracellular ROS.
423 This suggests that although both appear to target Mtb free thiols, there are differences in their
424 mechanisms. One hypothesis is that release of the phenyl-dioxopyrimidine group could also be
425 targeting a secondary unknown Mtb physiology, possibly explaining the higher ROS increase that
426 is observed compared to AC2P36 (Figure 4B). Both compounds also form adducts with the low
427 molecular weight thiol, GSH; however, there are major chemical scaffold differences. AC2P36
428 captures thiols with the release of methylsulfinate while AC2P20 is cleaved to generate
429 benzothioazole-mercaptoacetamide, which then goes on to form disulfide bonds. Although
430 AC2P20 and AC2P36 compounds are structurally unique and have distinct mechanisms-of-action,

431 they do exhibit similar physiological effects on Mtb, supporting the conclusion that thiol redox
432 homeostasis is specifically vulnerable to inhibition at acidic pH.

433 Several studies in Mtb show a link between low pH- and oxidative stress responses
434 [7,9,29,50,52]. At acidic pH *in vitro*, Mtb exhibits a more reduced cytoplasm and a shift from
435 glycolysis to fatty acid synthesis [9]. This metabolic remodeling is thought to occur in order to
436 generate more oxidized cofactors to mitigate reductive stress. However, a more reduced cytoplasm
437 in Mtb may also play a role in protecting Mtb against oxidative stress. A recent study comparing
438 the RNAseq profiles of reduced MSH redox potential (E_{MSH}-reduced), intraphagosmal Mtb, and
439 pH stress supports this claim and shows that E_{MSH}-reduced transcriptome has significant overlap
440 with the pH-regulon[50]. When we compare the E_{MSH}-reduced, intraphagosomal Mtb, and pH
441 stress regulons with AC2P20 and AC2P36 transcriptional profiles, we again see overlap in redox
442 sensitive genes (i.e. *katG*, *trxB2*, and *whiB3*) which are important for protection against oxidative
443 stress.

444 While both AC2P20 and AC2P36 share these similar gene induction characteristics, there
445 are differences in specific thiol-related genes. For example, methionine synthesis (i.e. *metK*, *metA*,
446 *metC*) appears modulated by AC2P36 treatment, but induction of these genes is absent in AC2P20
447 transcriptional data. Likewise, AC2P20 strongly induces sulfate reduction via APS (*cysH*, *nirA*),
448 however, these genes are not modulated by AC2P36. These differences may reflect differences in
449 how these compounds sequester free thiols and which free thiols in particular are being modified.
450 While mycothiol is the most abundant free thiol in Mtb (present in millimolar amounts) [53], it is
451 plausible AC2P20 targets other low molecular weight thiols such as ergothioneine (ERG) [32]
452 or gamma-glutamylcysteine (GGC) [54]. Our mass spectrometry data also supports AC2P20 may
453 be generally targeting free thiols, forming adducts with both GSH and NAC, which would indicate

454 that 1) AC2P20 can target a thiol group in general, and 2) it can directly target a cysteine derivative.
455 Further profiling experiments would need to be undertaken to determine in which molecular
456 contexts AC2P20 targets free thiols and indeed, other related molecules are being developed as
457 tools for cysteine-reactive profiling [45,46].
458
459 **Conclusions**
460 The discovery of two independent molecules selectively killing Mtb at acidic pH by
461 depleting free thiols provides further support for our hypothesis that Mtb is highly sensitive to thiol
462 homeostasis stress at acidic pH and this pathway is a valuable new target for TB drug discovery.
463 AC2P20 or AC2P36 in their present state, will not likely make useful drugs, as they could react
464 with host thiols and thus be neutralized prior to reaching Mtb or could be cytotoxic. However,
465 they independently point the way to further efforts to target this pathway. Indeed, the thioredoxin
466 reductase inhibitor auranofin is in early clinical trials to treat TB and acts, as shown here, similarly
467 functions by depleting free thiols, by a distinct, indirect mechanism. Several groups are pursuing
468 compounds that have enhanced killing at acidic pH but have mostly focused on bacterial pH-
469 homeostasis [16-18]. This new work further validates targeting thiol homeostasis as an alternative
470 target to kill Mtb at acidic pH. Other chemotypes, such as auranofin, that do so indirectly are likely
471 the most promising route. However, it could be possible to develop the compounds related to
472 AC2P20 or AC2P36 into prodrugs that are activated by a Mtb specific enzyme, thus releasing the
473 thiol-reactive warhead selectively inside the bacterial cell. Notably, for both AC2P20 and AC2P36
474 we could not isolate resistant mutants. This is consistent with the compounds having a broad target
475 (free thiols) and not a specific protein, where resistant mutants could be selected. Therefore, it is

476 possible that should a compound targeting free thiols be developed, the evolution of resistance
477 may be slower as compared to a traditional antibiotic.

478 In conclusion, our findings have uncovered a novel thiol-targeting chemical probe,
479 AC2P20. AC2P20, in combination with AC2P36, can be classified as a new class of compounds
480 that render Mtb especially sensitive to changes in thiol homeostasis at acidic pH. Further
481 experiments to examine the mechanism of this sensitivity can be undertaken using AC2P20 or
482 AC2P36 as chemical probes. For example, using TN-seq, identification of mutants that become
483 sensitive to AC2P20 and AC2P36 at a neutral pH or have enhanced sensitivity at acidic pH, may
484 reveal key functional pathways required for maintaining thiol-homeostasis.

485

486

487 **Conflicts of Interest**

488 R.B.A. is the founder and owner of Tarn Biosciences, Inc., a company that is working to develop
489 new TB drugs.

490

491 **Acknowledgements**

492 We thank Christopher Colvin and Javiera Ortiz for technical assistance on the high throughput
493 screening and cytoplasmic pH assays, respectively. Research on this project was supported grants
494 from the NIH-NIAID to RBA (U54AI057153, R01AI116605, R21AI105867) and
495 AgBioResearch.

496

497

498

499 **Author Contributions**

500 S.J.D., G.B.C., and R.B.A. conceived the project. S.J.D performed the time-dependent and
501 concentration-dependent killing assays, RNAseq analysis, mass spectrometry, free thiol assay, and
502 ROS assay. G.B.C. conducted the initial characterization studies including Mtb and *M. smegmatis*
503 EC_{50} assays and the RNAseq experiment. M.W.W. and S.D.L. contributed to mass spectrometry
504 analysis and proposed mechanism. S.J.D. and R.B.A. wrote the manuscript.

505

506

507 ***Figure legends***

508 **<u>Figure 1. AC2P20 inhibits Mtb growth in a pH-dependent manner.</u>**

509 A) The chemical structure of AC2P20 ((N-1,3-benzothiazol-2-yl-2-[(4,6-dioxo-5-phenyl-1,4,5,6-

510 tetrahydropyrimidin-2-yl)thio]acetamide)

511 B) Mtb growth is inhibited in a dose-dependent manner when treated with AC2P20 at pH 5.7 and

512 exhibits an EC_{50} of 4.3 μM following six days of treatment. Treatment with AC2P20 at pH 7.0

513 Mtb requires concentrations >60 μM to see growth inhibitory effects.

514 C) Mtb treated with 20 μM of AC2P20 and grown in buffered 7H9 media (pH 5.7) for 5 days

515 shows time-dependent killing as indicated by ~100-fold reduction in viability compared to the

516 DMSO control. Time-dependent killing is not observed in neutral conditions.

517 D) Mtb was treated with a dose-response of AC2P20 at pH 5.7 for 7 days, then assessed for

518 dose-dependent killing by plating for colony-forming units (CFUs). The dotted line indicates the

519 CFUs plated on Day 0.

520

521 **<u>Figure 2. AC2P20 treatment promotes a thiol-oxidative and redox stress response.</u>**

522 A) Mtb differential gene expression data after being treated for 24 hours with 20 μM AC2P20 at

523 pH 5.7. Genes indicated include those involved in sulfur metabolism, transcriptional regulation,

524 and redox homeostasis. Statistically significant genes ($q < 0.05$) are highlighted in red.

525 B) A pie chart depicting the functional classification breakdown of significantly induced genes

526 (>2-fold, $q < 0.05$) following the analysis of AC2P20-treated Mtb RNA-seq profile.

527 C) Heatmap comparing 16 upregulated genes (between AC2P20 and AC2P36 at pH 5.7 that are

528 involved in sulfur metabolism, transcriptional regulation, and redox homeostasis . Genes were

529 annotated with the H37Rv genome.

530 D) Venn diagrams comparing upregulated and downregulated gene overlap (>2-fold, $q < 0.05$)
531 between AC2P20-treated and AC2P36-treated Mtb [29].
532
533 **Figure 3. AC2P20 forms adducts with free thiols at acidic pH.**
534 A) AC2P20 was incubated in Tris-HCl buffer, pH 5.7 with reduced glutathione (GSH) for one
535 hour. An AC2P20-GSH adduct (~528 Da) was confirmed via mass spectrometry. Samples were
536 run in duplicate and observed in negative ESI mode.
537 B) In the absence of GSH, AC2P20 incubated with DMSO does not fragment at pH 5.7. Only the
538 parent molecule is observable at a molecular weight of ~409 Da. Samples were run in duplicate
539 and observed in negative ESI mode.
540 C) AC2P20-GSH adduct formation at pH 5.7 (~530 Da) was also observed in positive ESI mode,
541 as well as adduct loss of the glutamate fragment (~401 Da) and subsequent fragmentation of the
542 AC2P20 molecule and its pyrimidine fragments. Samples were run in duplicate.
543
544 **Figure 4. AC2P20 depletes free thiols and induces intracellular ROS accumulation.**
545 **A) Treatment of Mtb with AC2P20 leads to a pH-dependent decrease in free thiols.** Free thiol
546 depletion is observed at pH 5.7 with AC2P20 treatment. AC2P36 is a pH-dependent chemical
547 probe known to deplete free thiol pools and serves as a positive control. Statistical significance
548 was calculated using a two-way ANOVA (*$p<0.05$).
549 **B) ROS accumulate under AC2P20 treatment at acidic conditions.** Mtb treatment with
550 AC2P20 leads to a pH-dependent increase in intracellular reactive oxygen species (ROS). ROS
551 was detected using a final concentration of 5 μm fluorescent dye, CellROX Green, and normalized

552 to an OD_{595}. DMSO was used as a control. Statistical significance was calculated using a one-way
553 ANOVA (*$p<0.05$)
554
555 **Figure 5. Proposed mechanism for AC2P20 adduct formation.**
556 A) Proposed reaction mechanism for the formation of a disulfide bond between AC2P20 and GSH
557 at pH 5.7.
558 B) Proposed stable covalent bond formation between AC2P20 and free thiols in Mtb during redox
559 cycling.
560
561 **Supplemental Figures:**
562 **S1A.** Dose-response curve for AC2P20 inhibition of *M. smegmatis* GFP fluorescence.
563 **S1B.** AC2P20 does not modulate Mtb cytoplasmic pH at pH 5.7. DMSO and Nigericin served as
564 negative and positive controls, respectively.
565 **S1C.** The chemical structure of AC2P36 (5-chloro-N-(3-chloro-4-methoxyphenyl)-2-
566 methylsulfonylpyrimidine-4-carboxamide) [29].
567 **S2A.** A pie chart depicting the functional classification breakdown of significantly induced genes
568 (>2-fold, $q < 0.05$) following the analysis of AC2P36-treated Mtb RNA-seq profile.
569 **S2B.** Heatmap comparing the contrast between 8 differentially-regulated genes (between AC2P20
570 and AC2P36 at pH 5.7) that are involved in lipid metabolism and central metabolism. Genes were
571 annotated with the H37Rv genome.
572 **S3A.** Mass spectrometry data showing adduct formation between AC2P20 and GSH at pH 7.0.
573 Spectra were analyzed in negative ESI mode.

574 **S3B.** Mass spectrometry data showing adduct formation between AC2P20 and GSH at pH 8.5.
575 Spectra were analyzed in negative ESI mode.
576 **S3C.** AC2P20 incubated with DMSO does not fragment in the absence of GSH at pH 7.0. Spectra
577 were analyzed in negative ESI mode.
578 **S3D.** AC2P20 incubated with DMSO does not fragment in the absence of GSH at pH 8.5. Spectra
579 were analyzed in negative ESI mode.
580 **S4A.** Mass spectrometry data showing adduct formation between AC2P20 and N-acetylcysteine
581 at pH 5.7. Spectra were analyzed in negative ESI mode.
582 **S4B.** Mass spectrometry data showing adduct formation between AC2P20 and N-acetylcysteine
583 at pH 7.0. Spectra were analyzed in negative ESI mode. 20 +NAC 7.0
584 **S4C.** Mass spectrometry data showing adduct formation between AC2P20 and N-acetylcysteine
585 at pH 8.5. Spectra were analyzed in negative ESI mode.
586 **S4D.** AC2P20 is still able to form an adduct with GSH in the presence of the oxidant, H_2O_2. Spectra
587 were analyzed in negative ESI mode.
588 **S5.** A list of labeled mass spectrometry peaks with their corresponding hypothetical chemical
589 scaffolds.
590
591 **<u>Supplemental Table:</u>**
592 **Table S1:** Analyzed RNA-seq transcriptional profiling data. S1A. Classification of differentially
593 regulated genes. S1B. Genes significantly induced by AC2P20. S1C. Genes significantly repressed
594 by AC2P20. S1D. Complete list of unfiltered gene expression data in response to AC2P20
595 treatment.
596

597 ***References***

598 1. Dutta NK, Karakousis PC (2014) Latent tuberculosis infection: myths, models, and molecular
599 mechanisms. Microbiol Mol Biol Rev 78 (3):343-371. doi:10.1128/MMBR.00010-14

600 2. Rohde KH, Abramovitch RB, Russell DG (2007) Mycobacterium tuberculosis invasion of
601 macrophages: linking bacterial gene expression to environmental cues. Cell Host Microbe 2
602 (5):352-364. doi:10.1016/j.chom.2007.09.006

603 3. Baker JJ, Dechow SJ, Abramovitch RB (2019) Acid Fasting: Modulation of Mycobacterium
604 tuberculosis Metabolism at Acidic pH. Trends Microbiol 27 (11):942-953.
605 doi:10.1016/j.tim.2019.06.005

606 4. MacMicking JD, Taylor GA, McKinney JD (2003) Immune control of tuberculosis by IFN-
607 gamma-inducible LRG-47. Science 302 (5645):654-659. doi:10.1126/science.1088063

608 5. Vandal OH, Nathan CF, Ehrt S (2009) Acid resistance in Mycobacterium tuberculosis. J
609 Bacteriol 191 (15):4714-4721. doi:10.1128/JB.00305-09

610 6. Vandal OH, Pierini LM, Schnappinger D, Nathan CF, Ehrt S (2008) A membrane protein
611 preserves intrabacterial pH in intraphagosomal Mycobacterium tuberculosis. Nat Med 14
612 (8):849-854. doi:10.1038/nm.1795

613 7. Vandal OH, Roberts JA, Odaira T, Schnappinger D, Nathan CF, Ehrt S (2009) Acid-
614 susceptible mutants of Mycobacterium tuberculosis share hypersusceptibility to cell wall and
615 oxidative stress and to the host environment. J Bacteriol 191 (2):625-631. doi:10.1128/JB.00932-
616 08

617 8. Song H, Huff J, Janik K, Walter K, Keller C, Ehlers S, Bossmann SH, Niederweis M (2011)
618 Expression of the ompATb operon accelerates ammonia secretion and adaptation of
619 Mycobacterium tuberculosis to acidic environments. Mol Microbiol 80 (4):900-918.
620 doi:10.1111/j.1365-2958.2011.07619.x

621 9. Baker JJ, Johnson BK, Abramovitch RB (2014) Slow growth of Mycobacterium tuberculosis
622 at acidic pH is regulated by phoPR and host-associated carbon sources. Mol Microbiol 94 (1):56-
623 69. doi:10.1111/mmi.12688

624 10. Mehta M, Rajmani RS, Singh A (2016) Mycobacterium tuberculosis WhiB3 Responds to
625 Vacuolar pH-induced Changes in Mycothiol Redox Potential to Modulate Phagosomal
626 Maturation and Virulence. J Biol Chem 291 (6):2888-2903. doi:10.1074/jbc.M115.684597

627 11. Farhana A, Guidry L, Srivastava A, Singh A, Hondalus MK, Steyn AJ (2010) Reductive
628 stress in microbes: implications for understanding Mycobacterium tuberculosis disease and
629 persistence. Adv Microb Physiol 57 (C):43-117. doi:10.1016/B978-0-12-381045-8.00002-3

630 12. Abramovitch RB, Rohde KH, Hsu FF, Russell DG (2011) aprABC: a Mycobacterium
631 tuberculosis complex-specific locus that modulates pH-driven adaptation to the macrophage
632 phagosome. Mol Microbiol 80 (3):678-694. doi:10.1111/j.1365-2958.2011.07601.x

633 13. Singh A, Guidry L, Narasimhulu KV, Mai D, Trombley J, Redding KE, Giles GI, Lancaster
634 JR, Jr., Steyn AJ (2007) Mycobacterium tuberculosis WhiB3 responds to O2 and nitric oxide via
635 its [4Fe-4S] cluster and is essential for nutrient starvation survival. Proc Natl Acad Sci U S A
636 104 (28):11562-11567. doi:10.1073/pnas.0700490104

637 14. Singh A, Crossman DK, Mai D, Guidry L, Voskuil MI, Renfrow MB, Steyn AJ (2009)
638 Mycobacterium tuberculosis WhiB3 maintains redox homeostasis by regulating virulence lipid
639 anabolism to modulate macrophage response. PLoS Pathog 5 (8):e1000545.
640 doi:10.1371/journal.ppat.1000545

641 15. Baker JJ, Abramovitch RB (2018) Genetic and metabolic regulation of Mycobacterium
642 tuberculosis acid growth arrest. Sci Rep 8 (1):4168. doi:10.1038/s41598-018-22343-4

643 16. Zhao N, Darby CM, Small J, Bachovchin DA, Jiang X, Burns-Huang KE, Botella H, Ehrt S,
644 Boger DL, Anderson ED, Cravatt BF, Speers AE, Fernandez-Vega V, Hodder PS, Eberhart C,
645 Rosen H, Spicer TP, Nathan CF (2015) Target-based screen against a periplasmic serine protease
646 that regulates intrabacterial pH homeostasis in Mycobacterium tuberculosis. ACS Chem Biol 10
647 (2):364-371. doi:10.1021/cb500746z

648 17. Darby CM, Ingolfsson HI, Jiang X, Shen C, Sun M, Zhao N, Burns K, Liu G, Ehrt S, Warren
649 JD, Andersen OS, Brickner SJ, Nathan C (2013) Whole cell screen for inhibitors of pH
650 homeostasis in Mycobacterium tuberculosis. PLoS One 8 (7):e68942.
651 doi:10.1371/journal.pone.0068942

652 18. Early J, Ollinger J, Darby C, Alling T, Mullen S, Casey A, Gold B, Ochoada J, Wiernicki T,
653 Masquelin T, Nathan C, Hipskind PA, Parish T (2019) Identification of Compounds with pH-
654 Dependent Bactericidal Activity against Mycobacterium tuberculosis. ACS Infect Dis 5 (2):272-
655 280. doi:10.1021/acsinfecdis.8b00256

656 19. Reichlen MJ, Leistikow RL, Scobey MS, Born SEM, Voskuil MI (2017) Anaerobic
657 Mycobacterium tuberculosis Cell Death Stems from Intracellular Acidification Mitigated by the
658 DosR Regulon. J Bacteriol 199 (23). doi:10.1128/JB.00320-17

659 20. Tan MP, Sequeira P, Lin WW, Phong WY, Cliff P, Ng SH, Lee BH, Camacho L,
660 Schnappinger D, Ehrt S, Dick T, Pethe K, Alonso S (2010) Nitrate respiration protects hypoxic
661 Mycobacterium tuberculosis against acid- and reactive nitrogen species stresses. PLoS One 5
662 (10):e13356. doi:10.1371/journal.pone.0013356

663 21. Hards K, McMillan DGG, Schurig-Briccio LA, Gennis RB, Lill H, Bald D, Cook GM (2018)
664 Ionophoric effects of the antitubercular drug bedaquiline. Proc Natl Acad Sci U S A 115
665 (28):7326-7331. doi:10.1073/pnas.1803723115

666 22. Flentie K, Harrison GA, Tukenmez H, Livny J, Good JAD, Sarkar S, Zhu DX, Kinsella RL,
667 Weiss LA, Solomon SD, Schene ME, Hansen MR, Cairns AG, Kulen M, Wixe T, Lindgren
668 AEG, Chorell E, Bengtsson C, Krishnan KS, Hultgren SJ, Larsson C, Almqvist F, Stallings CL
669 (2019) Chemical disarming of isoniazid resistance in Mycobacterium tuberculosis. Proc Natl
670 Acad Sci U S A 116 (21):10510-10517. doi:10.1073/pnas.1818009116

671 23. Harbut MB, Vilcheze C, Luo X, Hensler ME, Guo H, Yang B, Chatterjee AK, Nizet V,
672 Jacobs WR, Jr., Schultz PG, Wang F (2015) Auranofin exerts broad-spectrum bactericidal
673 activities by targeting thiol-redox homeostasis. Proc Natl Acad Sci U S A 112 (14):4453-4458.
674 doi:10.1073/pnas.1504022112

675 24. Lin K, O'Brien KM, Trujillo C, Wang R, Wallach JB, Schnappinger D, Ehrt S (2016)
676 Mycobacterium tuberculosis Thioredoxin Reductase Is Essential for Thiol Redox Homeostasis
677 but Plays a Minor Role in Antioxidant Defense. PLoS Pathog 12 (6):e1005675.
678 doi:10.1371/journal.ppat.1005675

679 25. Perez E, Samper S, Bordas Y, Guilhot C, Gicquel B, Martin C (2001) An essential role for
680 phoP in Mycobacterium tuberculosis virulence. Mol Microbiol 41 (1):179-187.
681 doi:10.1046/j.1365-2958.2001.02500.x

682 26. Gonzalo-Asensio J, Mostowy S, Harders-Westerveen J, Huygen K, Hernández-Pando R,
683 Thole J, Behr M, Gicquel B, Martín C (2008) PhoP: A Missing Piece in the Intricate Puzzle of
684 Mycobacterium tuberculosis Virulence. PLOS ONE 3 (10):e3496.
685 doi:10.1371/journal.pone.0003496

686 27. Walters SB, Dubnau E, Kolesnikova I, Laval F, Daffe M, Smith I (2006) The
687 Mycobacterium tuberculosis PhoPR two-component system regulates genes essential for
688 virulence and complex lipid biosynthesis. Mol Microbiol 60 (2):312-330. doi:10.1111/j.1365-
689 2958.2006.05102.x

690 28. Johnson BK, Colvin CJ, Needle DB, Mba Medie F, Champion PA, Abramovitch RB (2015)
691 The Carbonic Anhydrase Inhibitor Ethoxzolamide Inhibits the Mycobacterium tuberculosis
692 PhoPR Regulon and Esx-1 Secretion and Attenuates Virulence. Antimicrob Agents Chemother
693 59 (8):4436-4445. doi:10.1128/AAC.00719-15

694 29. Coulson GB, Johnson BK, Zheng H, Colvin CJ, Fillinger RJ, Haiderer ER, Hammer ND,
695 Abramovitch RB (2017) Targeting Mycobacterium tuberculosis Sensitivity to Thiol Stress at
696 Acidic pH Kills the Bacterium and Potentiates Antibiotics. Cell Chem Biol 24 (8):993-1004
697 e1004. doi:10.1016/j.chembiol.2017.06.018

698 30. Johnson BK, Scholz MB, Teal TK, Abramovitch RB (2016) SPARTA: Simple Program for
699 Automated reference-based bacterial RNA-seq Transcriptome Analysis. BMC Bioinformatics
700 17:66. doi:10.1186/s12859-016-0923-y

701 31. Purdy GE, Niederweis M, Russell DG (2009) Decreased outer membrane permeability
702 protects mycobacteria from killing by ubiquitin-derived peptides. Mol Microbiol 73 (5):844-857.
703 doi:10.1111/j.1365-2958.2009.06801.x

704 32. Saini V, Cumming BM, Guidry L, Lamprecht DA, Adamson JH, Reddy VP, Chinta KC,
705 Mazorodze JH, Glasgow JN, Richard-Greenblatt M, Gomez-Velasco A, Bach H, Av-Gay Y, Eoh
706 H, Rhee K, Steyn AJC (2016) Ergothioneine Maintains Redox and Bioenergetic Homeostasis
707 Essential for Drug Susceptibility and Virulence of Mycobacterium tuberculosis. Cell Rep 14
708 (3):572-585. doi:10.1016/j.celrep.2015.12.056

709 33. Williams JT, Haiderer ER, Coulson GB, Conner KN, Ellsworth E, Chen C, Alvarez-Cabrera
710 N, Li W, Jackson M, Dick T, Abramovitch RB (2019) Identification of New MmpL3 Inhibitors
711 by Untargeted and Targeted Mutant Screens Defines MmpL3 Domains with Differential
712 Resistance. Antimicrob Agents Chemother 63 (10). doi:10.1128/AAC.00547-19

713 34. Zheng H, Colvin CJ, Johnson BK, Kirchhoff PD, Wilson M, Jorgensen-Muga K, Larsen SD,
714 Abramovitch RB (2017) Inhibitors of Mycobacterium tuberculosis DosRST signaling and
715 persistence. Nat Chem Biol 13 (2):218-225. doi:10.1038/nchembio.2259

716 35. Kapopoulou A, Lew JM, Cole ST (2011) The MycoBrowser portal: a comprehensive and
717 manually annotated resource for mycobacterial genomes. Tuberculosis (Edinb) 91 (1):8-13.
718 doi:10.1016/j.tube.2010.09.006

719 36. Voskuil MI, Bartek IL, Visconti K, Schoolnik GK (2011) The response of mycobacterium
720 tuberculosis to reactive oxygen and nitrogen species. Front Microbiol 2:105.
721 doi:10.3389/fmicb.2011.00105

722 37. Manganelli R, Voskuil MI, Schoolnik GK, Dubnau E, Gomez M, Smith I (2002) Role of the
723 extracytoplasmic-function sigma factor sigma(H) in Mycobacterium tuberculosis global gene
724 expression. Mol Microbiol 45 (2):365-374. doi:10.1046/j.1365-2958.2002.03005.x

725 38. Raman S, Song T, Puyang X, Bardarov S, Jacobs WR, Jr., Husson RN (2001) The alternative
726 sigma factor SigH regulates major components of oxidative and heat stress responses in
727 Mycobacterium tuberculosis. J Bacteriol 183 (20):6119-6125. doi:10.1128/JB.183.20.6119-
728 6125.2001

729 39. Voss M, Nimtz M, Leimkuhler S (2011) Elucidation of the dual role of Mycobacterial
730 MoeZR in molybdenum cofactor biosynthesis and cysteine biosynthesis. PLoS One 6
731 (11):e28170. doi:10.1371/journal.pone.0028170

732 40. Warrier T, Kapilashrami K, Argyrou A, Ioerger TR, Little D, Murphy KC, Nandakumar M,
733 Park S, Gold B, Mi J, Zhang T, Meiler E, Rees M, Somersan-Karakaya S, Porras-De Francisco
734 E, Martinez-Hoyos M, Burns-Huang K, Roberts J, Ling Y, Rhee KY, Mendoza-Losana A, Luo
735 M, Nathan CF (2016) N-methylation of a bactericidal compound as a resistance mechanism in
736 Mycobacterium tuberculosis. Proc Natl Acad Sci U S A 113 (31):E4523-4530.
737 doi:10.1073/pnas.1606590113

738 41. Sun Z, Cheng SJ, Zhang H, Zhang Y (2001) Salicylate uniquely induces a 27-kDa protein in
739 tubercle bacillus. FEMS Microbiol Lett 203 (2):211-216. doi:10.1111/j.1574-
740 6968.2001.tb10843.x

741 42. Cole ST, Brosch R, Parkhill J, Garnier T, Churcher C, Harris D, Gordon SV, Eiglmeier K,
742 Gas S, Barry CE, 3rd, Tekaia F, Badcock K, Basham D, Brown D, Chillingworth T, Connor R,
743 Davies R, Devlin K, Feltwell T, Gentles S, Hamlin N, Holroyd S, Hornsby T, Jagels K, Krogh A,
744 McLean J, Moule S, Murphy L, Oliver K, Osborne J, Quail MA, Rajandream MA, Rogers J,
745 Rutter S, Seeger K, Skelton J, Squares R, Squares S, Sulston JE, Taylor K, Whitehead S, Barrell
746 BG (1998) Deciphering the biology of Mycobacterium tuberculosis from the complete genome
747 sequence. Nature 393 (6685):537-544. doi:10.1038/31159

748 43. Garbe TR (2004) Co-induction of methyltransferase Rv0560c by naphthoquinones and fibric
749 acids suggests attenuation of isoprenoid quinone action in Mycobacterium tuberculosis. Can J
750 Microbiol 50 (10):771-778. doi:10.1139/w04-067

751 44. Camus JC, Pryor MJ, Medigue C, Cole ST (2002) Re-annotation of the genome sequence of
752 Mycobacterium tuberculosis H37Rv. Microbiology 148 (Pt 10):2967-2973.
753 doi:10.1099/00221287-148-10-2967

754 45. Motiwala HF, Kuo YH, Stinger BL, Palfey BA, Martin BR (2020) Tunable Heteroaromatic
755 Sulfones Enhance in-Cell Cysteine Profiling. J Am Chem Soc 142 (4):1801-1810.
756 doi:10.1021/jacs.9b08831

757 46. Zambaldo C, Vinogradova EV, Qi X, Iaconelli J, Suciu RM, Koh M, Senkane K, Chadwick
758 SR, Sanchez BB, Chen JS, Chatterjee AK, Liu P, Schultz PG, Cravatt BF, Bollong MJ (2020) 2-
759 Sulfonylpyridines as Tunable, Cysteine-Reactive Electrophiles. J Am Chem Soc 142 (19):8972-
760 8979. doi:10.1021/jacs.0c02721

761 47. Murphy CM, Fenselau C, Gutierrez PL (1992) Fragmentation characteristic of glutathione
762 conjugates activated by high-energy collisions. J Am Soc Mass Spectrom 3 (8):815-822.
763 doi:10.1016/1044-0305(92)80004-5

764 48. Fine Z, Wood TD (2013) Formation of Mercury(II)-Glutathione Conjugates Examined Using
765 High Mass Accuracy Mass Spectrometry. Int J Anal Mass Spectrom Cromatogr 1 (2):90-94.
766 doi:10.4236/ijamsc.2013.12011

767 49. Abedinzadeh Z, Gardes-Albert M, Ferradini C (1989) Kinetic study of the oxidation
768 mechanism of glutathione by hydrogen peroxide in neutral aqueous medium. Canadian Journal
769 of Chemistry 67:1247-1255

770 50. Mishra R, Kohli S, Malhotra N, Bandyopadhyay P, Mehta M, Munshi M, Adiga V, Ahuja
771 VK, Shandil RK, Rajmani RS, Seshasayee ASN, Singh A (2019) Targeting redox heterogeneity
772 to counteract drug tolerance in replicating Mycobacterium tuberculosis. Sci Transl Med 11 (518).
773 doi:10.1126/scitranslmed.aaw6635

774 51. Ruth MM, van Rossum M, Koeken V, Pennings LJ, Svensson EM, Ruesen C, Bowles EC,
775 Wertheim HFL, Hoefsloot W, van Ingen J (2019) Auranofin Activity Exposes Thioredoxin
776 Reductase as a Viable Drug Target in Mycobacterium abscessus. Antimicrob Agents Chemother
777 63 (9). doi:10.1128/AAC.00449-19

778 52. Small JL, O'Donoghue AJ, Boritsch EC, Tsodikov OV, Knudsen GM, Vandal O, Craik CS,
779 Ehrt S (2013) Substrate specificity of MarP, a periplasmic protease required for resistance to acid
780 and oxidative stress in Mycobacterium tuberculosis. J Biol Chem 288 (18):12489-12499.
781 doi:10.1074/jbc.M113.456541

782 53. Newton GL, Arnold K, Price MS, Sherrill C, Delcardayre SB, Aharonowitz Y, Cohen G,
783 Davies J, Fahey RC, Davis C (1996) Distribution of thiols in microorganisms: mycothiol is a
784 major thiol in most actinomycetes. J Bacteriol 178 (7):1990-1995. doi:10.1128/jb.178.7.1990-
785 1995.1996

786 54. Sao Emani C, Williams MJ, Van Helden PD, Taylor MJC, Wiid IJ, Baker B (2018) Gamma-
787 glutamylcysteine protects ergothioneine-deficient Mycobacterium tuberculosis mutants against
788 oxidative and nitrosative stress. Biochem Biophys Res Commun 495 (1):174-178.
789 doi:10.1016/j.bbrc.2017.10.163
790

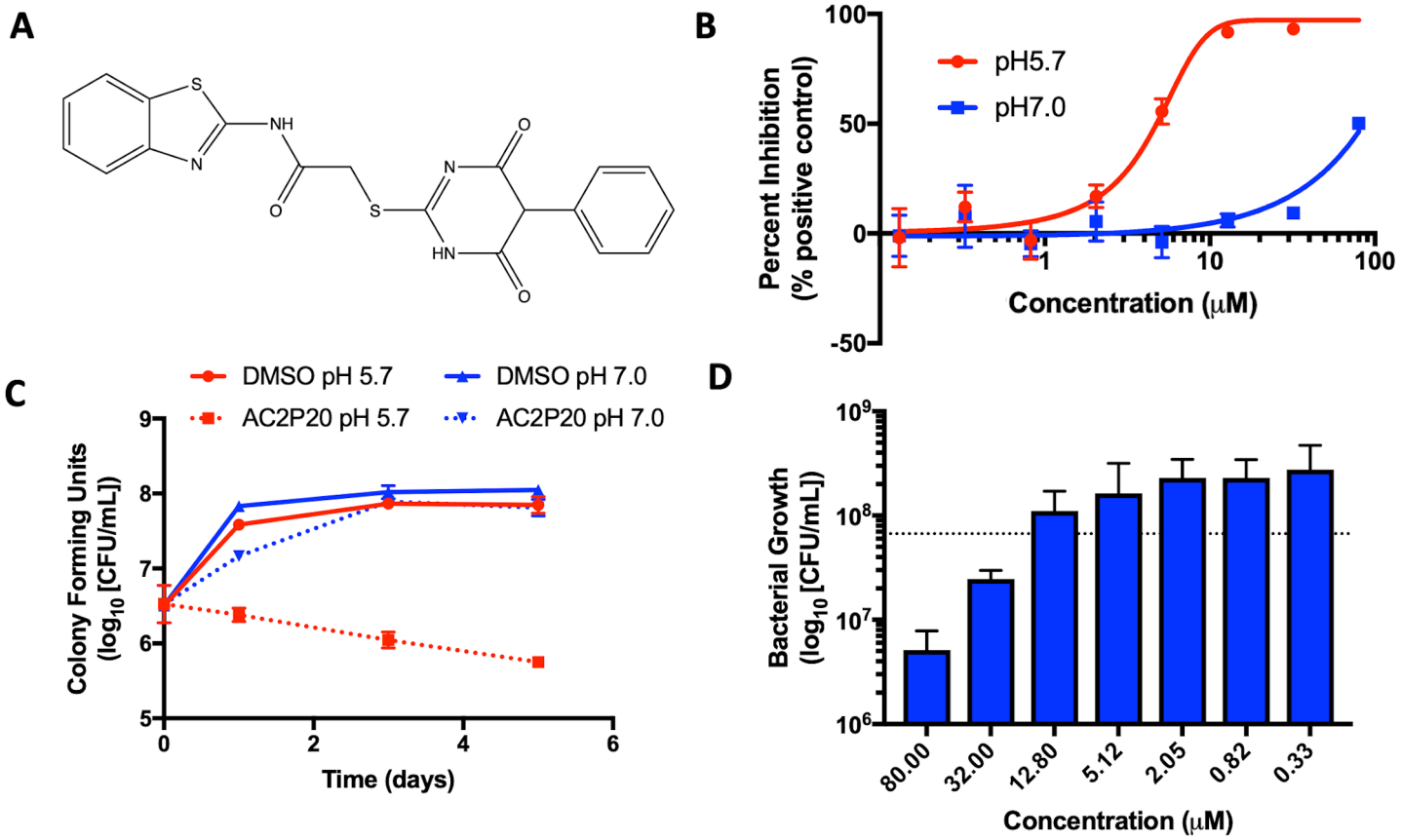
A
S
NH
N
O
S
N
O
HN
O
B
100
50
0
-50
Percent Inhibition
(% positive control)
pH5.7
pH7.0
1
10
100
Concentration (μM)
C
DMSO pH 5.7
DMSO pH 7.0
AC2P20 pH 5.7
AC2P20 pH 7.0
9
8
7
6
5
Colony Forming Units
(log10 [CFU/mL])
0
2
4
6
Time (days)
D
10^9
10^8
10^7
10^6
Bacterial Growth
(log10 [CFU/mL])
80.00
32.00
12.80
5.12
2.05
0.82
0.33
Concentration (μM)

Figure 1

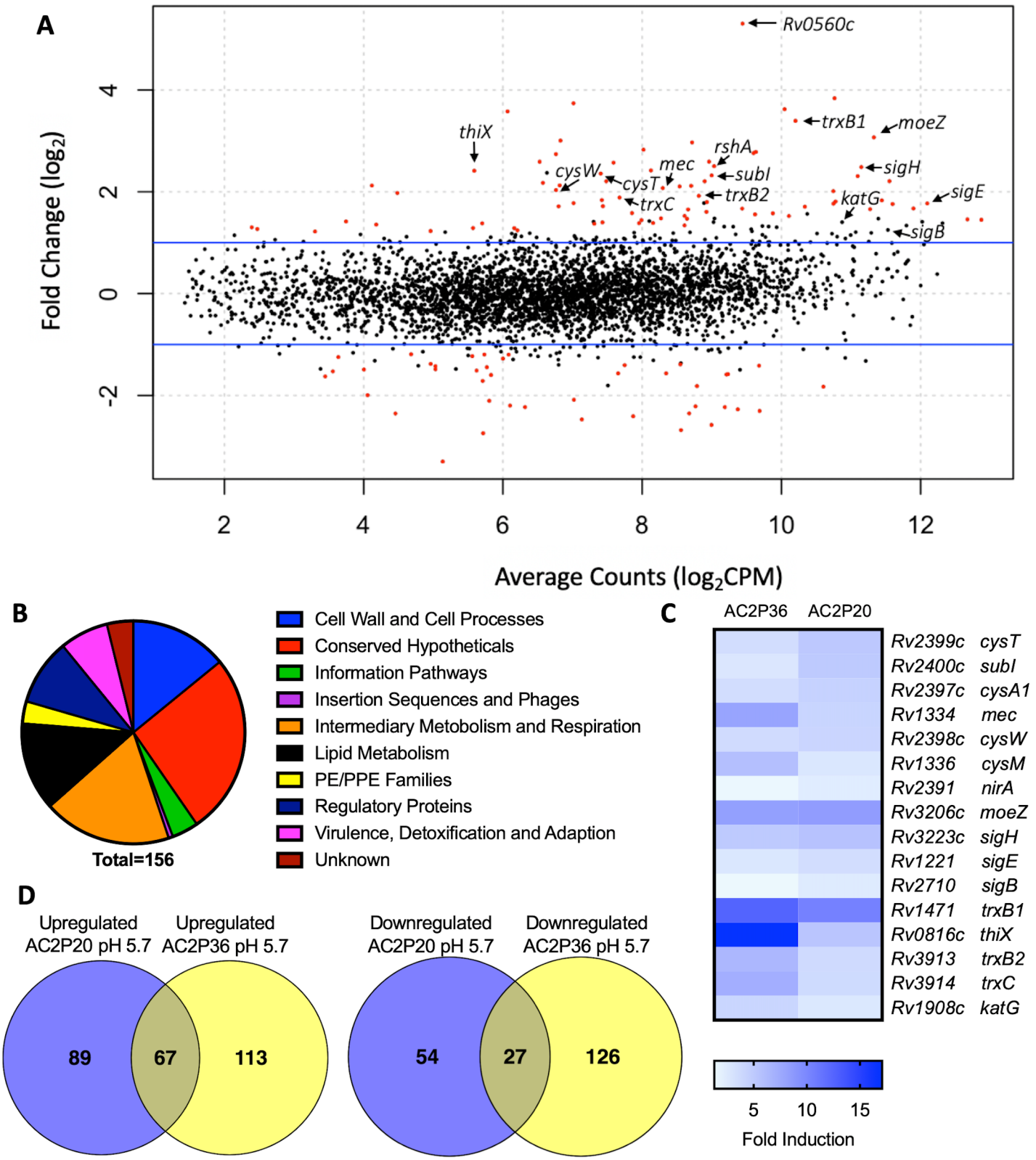
A
Rv0560c
trxB1
moeZ
thiX
rshA
mec
sigH
cysW
cysT
subI
trxB2
katG
sigE
trxC
sigB
Fold Change (log2)
Average Counts (log2CPM)
B
Cell Wall and Cell Processes
Conserved Hypotheticals
Information Pathways
Insertion Sequences and Phages
Intermediary Metobolism and Respiration
Lipid Metabolism
PE/PPE Families
Regulatory Proteins
Virulence, Detoxification and Adaption
Unknown
Total=156
C
AC2P36
AC2P20
Rv2399c cysT
Rv2400c subI
Rv2397c cysA1
Rv1334 mec
Rv2398c cysW
Rv1336 cysM
Rv2391 nirA
Rv3206c moeZ
Rv3223c sigH
Rv1221 sigE
Rv2710 sigB
Rv1471 trxB1
Rv0816c thiX
Rv3913 trxB2
Rv3914 trxC
Rv1908c katG
Fold Induction
D
Upregulated AC2P20 pH 5.7
Upregulated AC2P36 pH 5.7
89
67
113
Downregulated AC2P20 pH 5.7
Downregulated AC2P36 pH 5.7
54
27
126

Figure 2

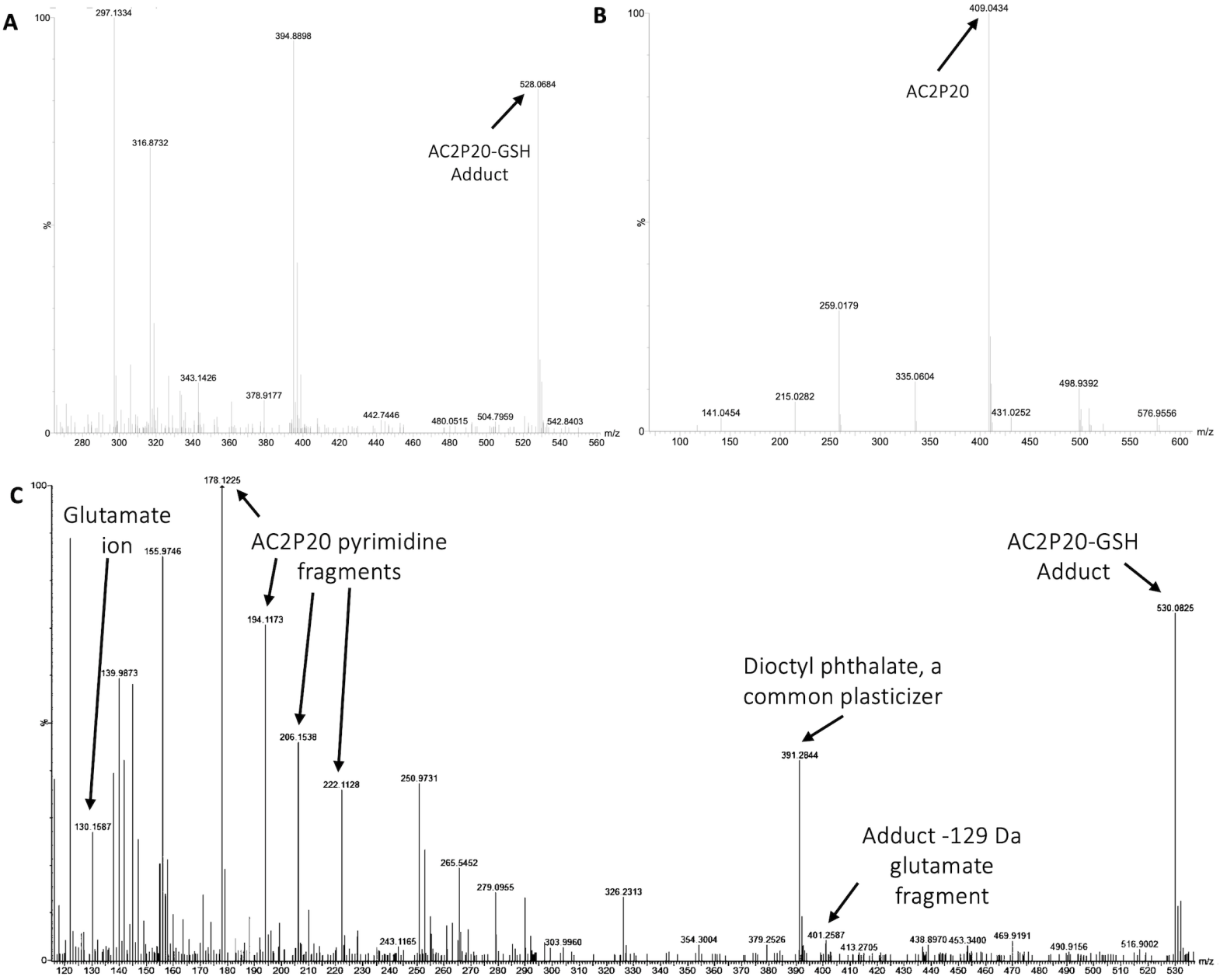
A
297.1334
394.8898
316.8732
528.0684
AC2P20-GSH
Adduct
343.1426
378.9177
442.7446
480.0515
504.7959
542.8403
m/z
B
409.0434
AC2P20
259.0179
335.0604
498.9392
215.0282
141.0454
431.0252
576.9556
m/z
C
Glutamate
ion
178.1225
155.9746
AC2P20 pyrimidine
fragments
194.1173
139.9873
206.1538
222.1128
250.9731
130.1587
265.5452
279.0955
326.2313
243.1165
303.9960
354.3004
379.2526
401.2587
413.2705
438.8970
453.3400
469.9191
490.9156
516.9002
AC2P20-GSH
Adduct
530.0825
Dioctyl phthalate, a
common plasticizer
391.2844
Adduct -129 Da
glutamate
fragment
m/z

Figure 3

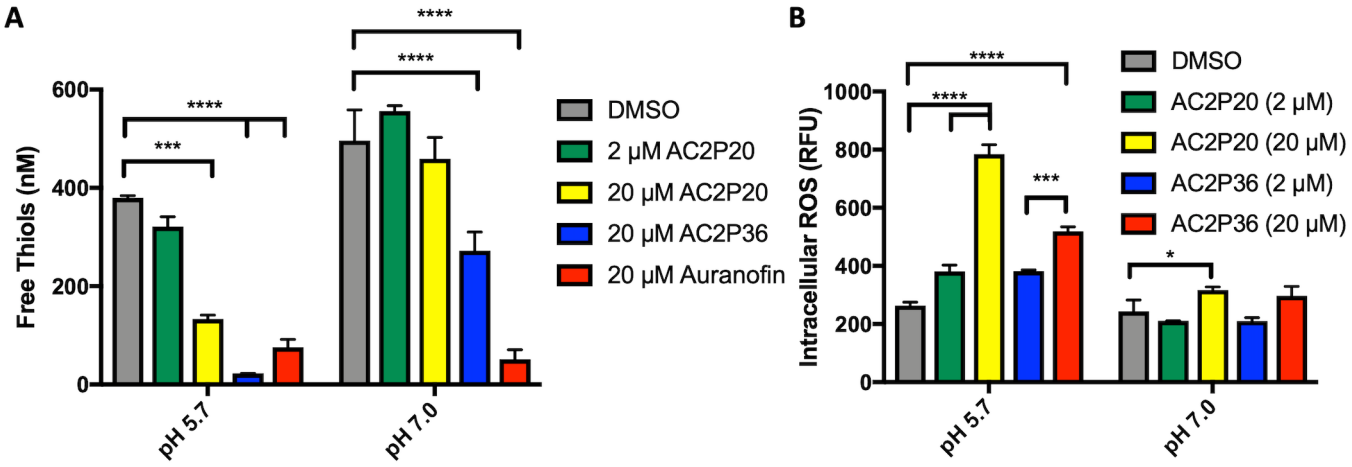
A
Free Thiols (nM)
600
400
200
0
****
***
****
****
pH 5.7
pH 7.0
DMSO
2 μM AC2P20
20 μM AC2P20
20 μM AC2P36
20 μM Auranofin
B
Intracellular ROS (RFU)
1000
800
600
400
200
0
****
****
***
*
pH 5.7
pH 7.0
DMSO
AC2P20 (2 μM)
AC2P20 (20 μM)
AC2P36 (2 μM)
AC2P36 (20 μM)

Figure 4

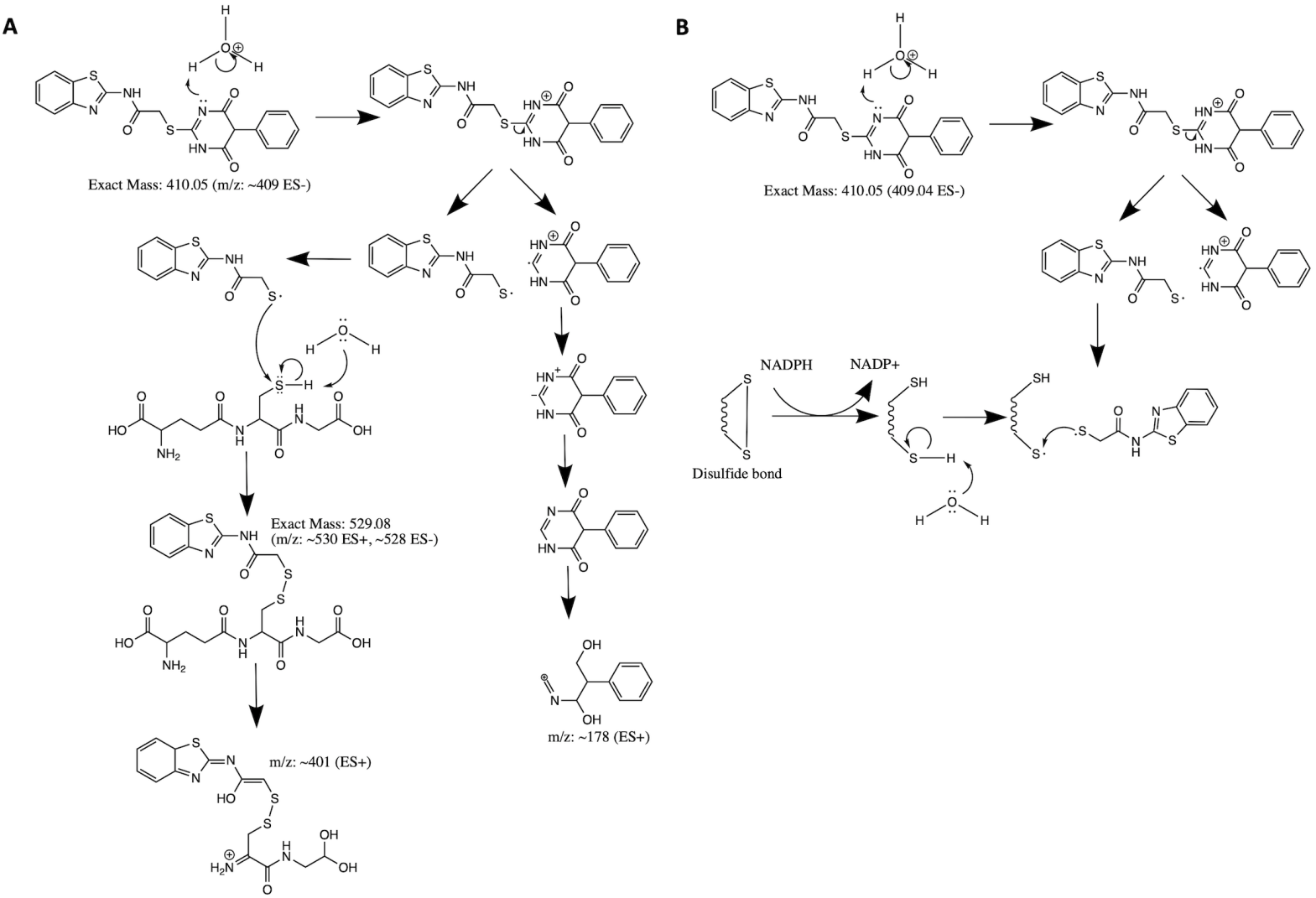
A
Exact Mass: 410.05 (m/z: ~409 ES-)
Exact Mass: 529.08
(m/z: ~530 ES+, ~528 ES-)
m/z: ~401 (ES+)
m/z: ~178 (ES+)
B
Exact Mass: 410.05 (409.04 ES-)
NADPH
NADP+
Disulfide bond

Figure 5

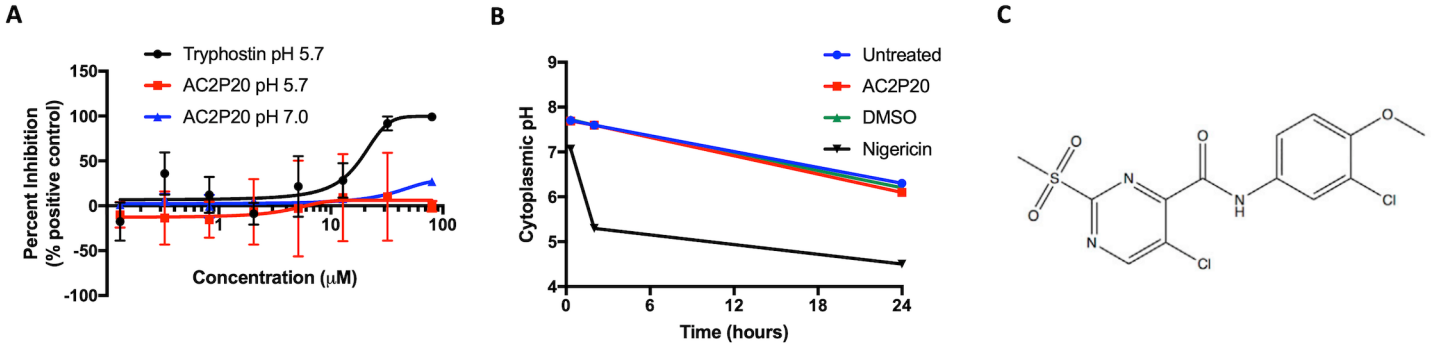

Supplemental Figure 1

A

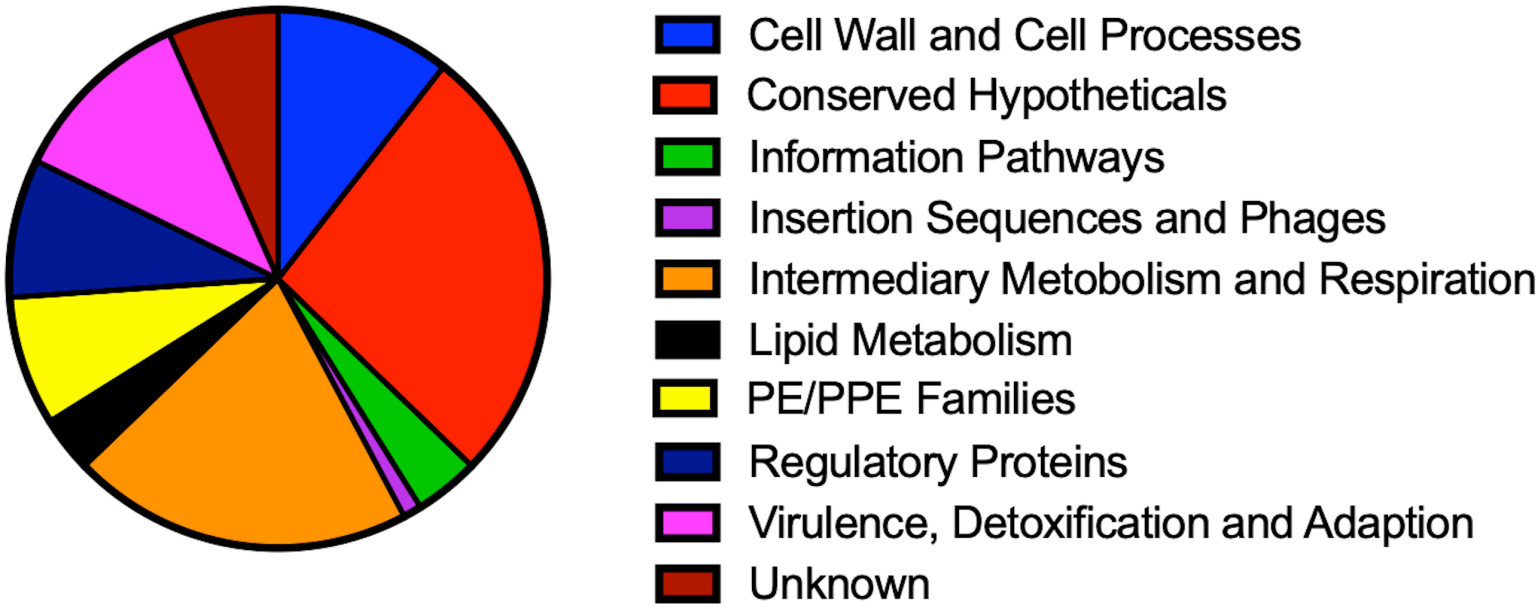

Total=180

B

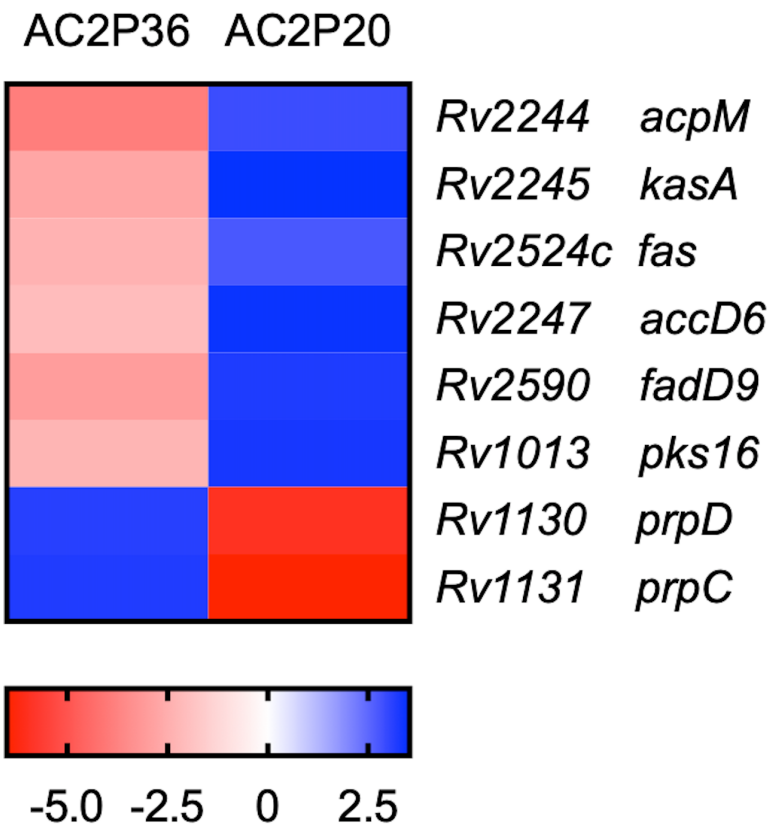

Supplemental Figure 2

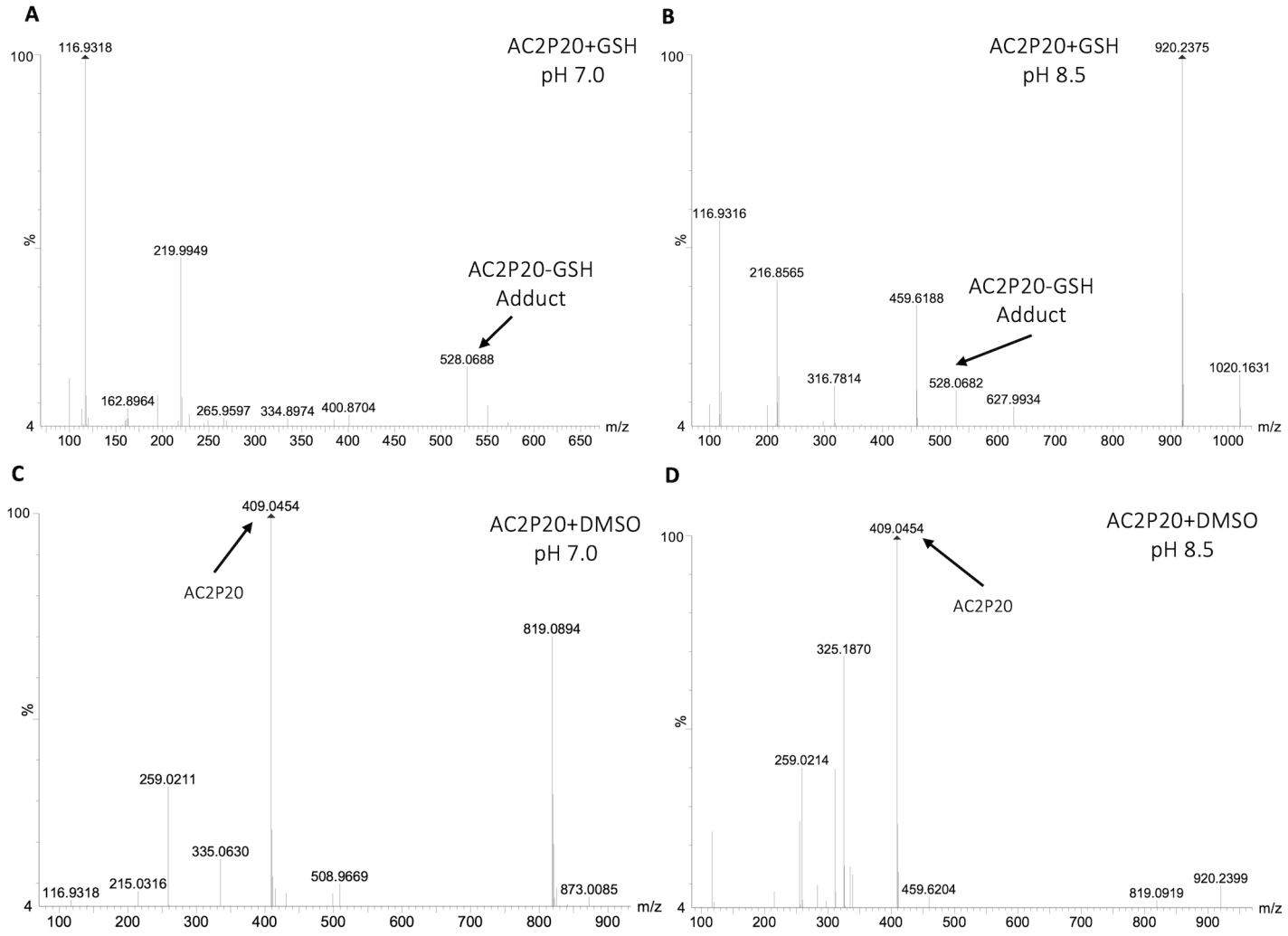

Supplemental Figure 3

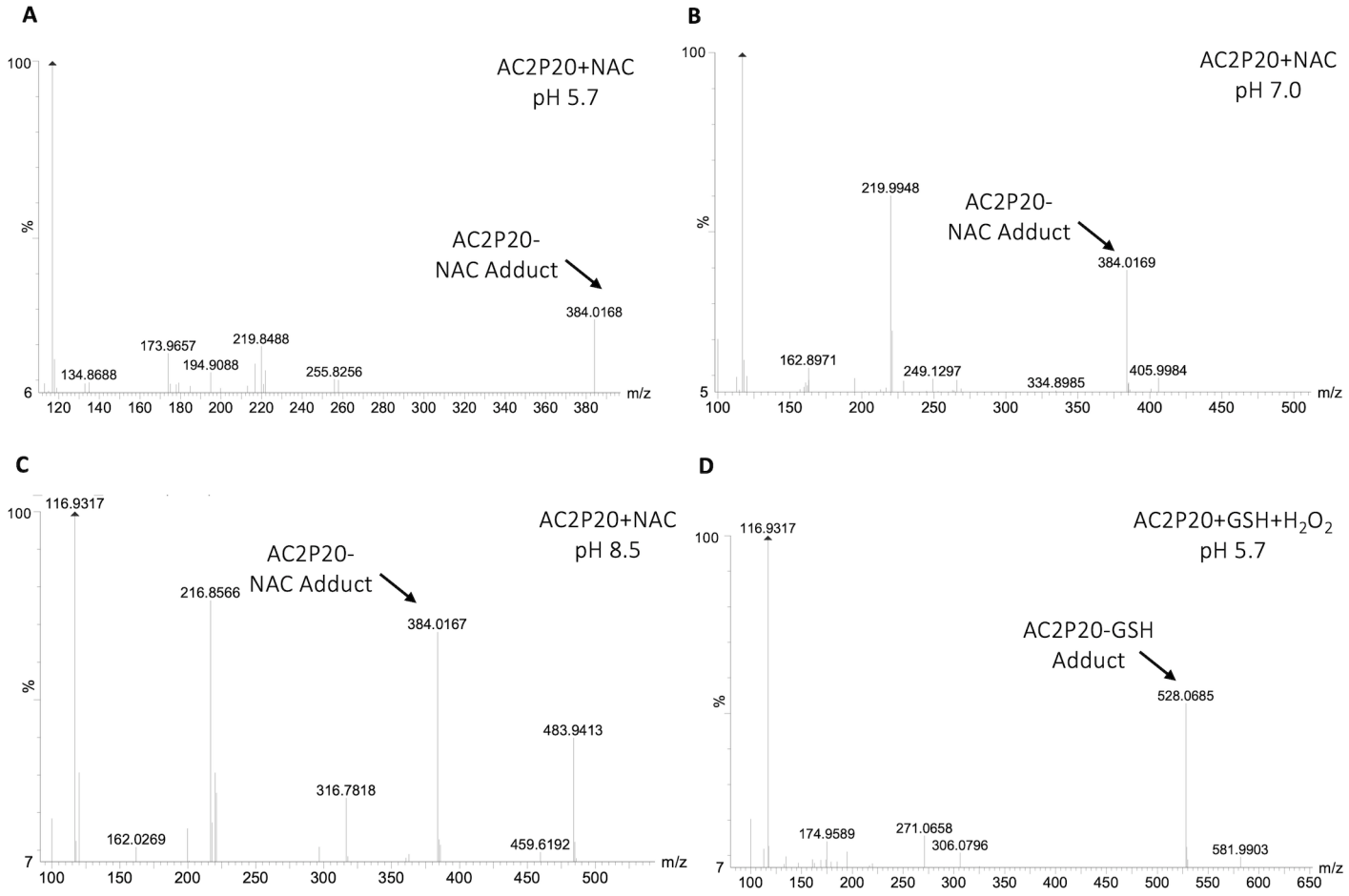

Supplemental Figure 4

Peak (Da)	Possible Chemical Scaffold	Figure No.
130.16	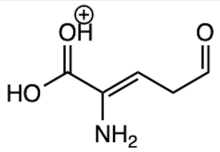	3C
178.12	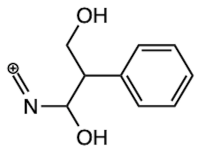	3C
194.12	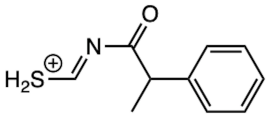	3C
206.15	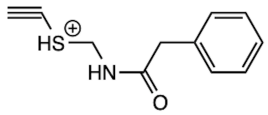	3C
222.11	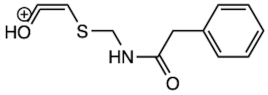	3C
384.02	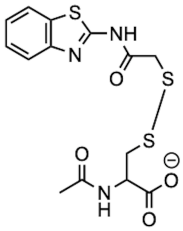	S3A, S3B, S3C
391.28	Phthalate Plasticizer	3C
401.26	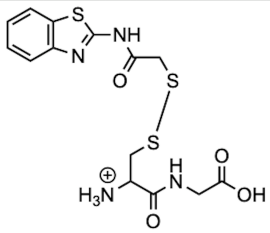	3C
409.04, 409.05	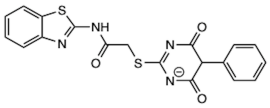	3B, S2C, S2D,
528.06, 528.07	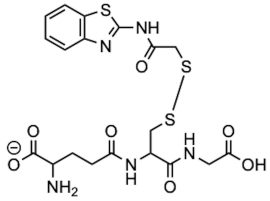	3A, S2A, S2B, S3D
530.08	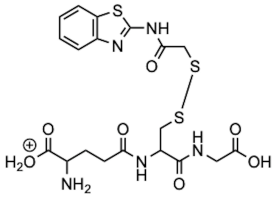	3C

Supplemental Figure 5

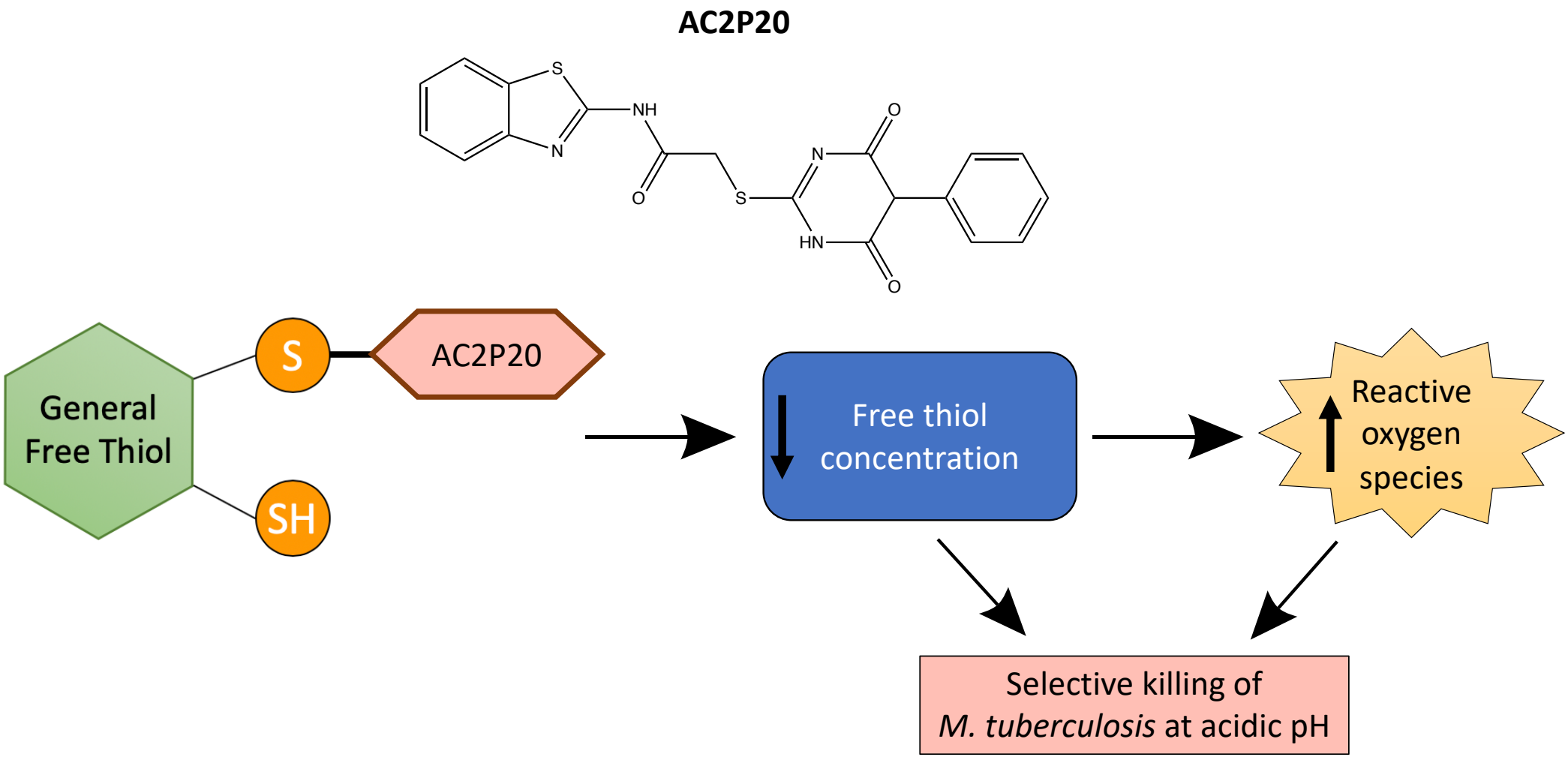
AC2P20
S
NH
N
O
S
N
O
HN
O
General Free Thiol
S
SH
AC2P20
Free thiol concentration
Reactive oxygen species
Selective killing of *M. tuberculosis* at acidic pH